CARDIFF UNIVERSITY
PRIFYSGOL CAERDYDD

# ORCA – Online Research @ Cardiff

This is an Open Access document downloaded from ORCA, Cardiff University's institutional repository:https://orca.cardiff.ac.uk/id/eprint/142925/

This is the author's version of a work that was submitted to / accepted for publication.

Citation for final published version:

Bailes, M., Berger, B. K., Brady, P. R., Branchesi, M., Danzmann, K., Evans, M., Holley-Bockelmann, K., Iyer, B. R., Kajita, T., Katsanevas, S., Kramer, M., Lazzarini, A., Lehner, L., Losurdo, G., Lück, H., McClelland, D. E., McLaughlin, M. A., Punturo, M., Ransom, S., Raychaudhury, S., Reitze, D. H., Ricci, F., Rowan, S., Saito, Y., Sanders, G. H., Sathyaprakash, B. S., Schutz, B. F. , Sesana, A., Shinkai, H., Siemens, X., Shoemaker, D. H., Thorpe, J., van den Brand, J. F. J. and Vitale, S. 2021. Gravitational-wave physics and astronomy in the 2020s and 2030s. Nature Reviews Physics 3 (5) , 344–366. 10.1038/s42254-021-00303-8

Publishers page: http://dx.doi.org/10.1038/s42254-021-00303-8

Please note:
Changes made as a result of publishing processes such as copy-editing, formatting and page numbers may not be reflected in this version. For the definitive version of this publication, please refer to the published source. You are advised to consult the publisher's version if you wish to cite this paper.

This version is being made available in accordance with publisher policies. See http://orca.cf.ac.uk/policies.html for usage policies. Copyright and moral rights for publications made available in ORCA are retained by the copyright holders.

# Gravitational-Wave Physics and Astronomy in the 2020s and 2030s

M. Bailes,[1,2] B. K. Berger,[3] P. R. Brady,[4] M. Branchesi,[5,6] K. Danzmann,[7,8] M. Evans,[9] K. Holley-Bockelmann,[10,11] B. R. Iyer,[12] T. Kajita,[13] S Katsanevas,[14] M. Kramer,[15,16] A. Lazzarini,[17] L. Lehner,[18] G. Losurdo,[19] H. Lück,[7,8] D. E. McClelland,[20] M. Punturo,[21] S. Ransom,[22] S. Raychaudhury,[23] D. H. Reitze,[17,24] F. Ricci,[25,26] S. Rowan,[27] Y. Saito,[28,29] G. H. Sanders,[30] B. S. Sathyaprakash,[31,32] B. F. Schutz,[32] A. Sesana,[33] H. Shinkai,[34] X. Siemens,[4] D. H. Shoemaker,[9] J. Thorpe,[35] J. F. J. van den Brand,[36,37] and S. Vitale[38]

[1] *Centre for Astrophysics and Supercomputing, Swinburne University of Technology, P.O. Box 218, Hawthorn, Victoria 3122, Australia*

[2] *OzGrav, Australian National University, Canberra, Australian Capital Territory 0200, Australia*

[3] *Stanford University, Stanford, CA 94305, USA*

[4] *University of Wisconsin-Milwaukee, Milwaukee, WI 53201, USA*

[5] *Gran Sasso Science Institute (GSSI), I-67100 L'Aquila*

[6] *INFN, Laboratori Nazionali del Gran Sasso, I-67100 Assergi*

[7] *Leibniz Universität Hannover, D-30167 Hannover, Germany*

[8] *Max Planck Institute for Gravitational Physics (Albert Einstein Institute), D-30167 Hannover, Germany*

[9] *LIGO, Massachusetts Institute of Technology, Cambridge, MA 02139*

[10] *Vanderbilt University, Nashville, TN, USA*

[11] *Fisk University, Nashville, TN, USA*

[12] *International Centre for Theoretical Sciences, Tata Institute of Fundamental Research, Bengaluru 560089, India*

[13] *Institute for Cosmic Ray Research, the University of Tokyo, Kashiwa, Chiba 277-8582, Japan*

[14] *European Gravitational Observatory (EGO), I-56021 S. Stefano a Macerata (Pisa), Italy*

[15] *Max-Planck-Institut für Radioastronomie, Auf dem Hügel 69, 53121 Bonn, Germany*

[16] *Jodrell Bank Centre for Astrophysics, School of Physics and Astronomy,*

*University of Manchester, Manchester M13 9PL, UK*

[17] *LIGO, California Institute of Technology, Pasadena, CA 91125, USA*

[18] *Perimeter Institute for Theoretical Physics, Waterloo, ON N2L 2Y5, Canada*

[19] *INFN, Sezione di Pisa, I-56127 Pisa, Italy*

[20] *OzGrav, Centre for Gravitational Astrophysics,*
*Australian National University, Canberra,*
*Australian Capital Territory 0200, Australia*

[21] *INFN, Sezione di Perugia, I-06123 Perugia, Italy*

[22] *NRAO, 520 Edgemont Rd., Charlottesville, VA 22903, USA*

[23] *Inter-University Centre for Astronomy and Astrophysics (IUCAA), Pune 411007, India*

[24] *University of Florida, Gainesville, FL 32611, USA*

[25] *Università di Roma "La Sapienza," I-00185 Roma, Italy*

[26] *INFN, Sezione di Roma, I-00185 Roma, Italy*

[27] *SUPA, University of Glasgow, Glasgow G12 8QQ, United Kingdom*

[28] *Institute for Cosmic Ray Research,*
*the University of Tokyo, Kashiwa, Chiba, 277-8582, Japan*

[29] *High Energy Accelerator Research Organization (KEK), Tsukuba, Ibaraki 305-0801, Japan*

[30] *TMT Observatory Corporation, 1111 S. Arroyo Pkwy.,*
*Ste. 200, Pasadena, CA 91125, USA.*

[31] *The Pennsylvania State University, University Park, PA 16802, USA*

[32] *Cardiff University, Cardiff CF24 3AA, United Kingdom*

[33] *Università Degli Studi di Milano-Bicocca, Milan, Italy*

[34] *Osaka Institute of Technology, Hirakata, Osaka 573-0197, Japan*

[35] *Gravitational Astrophysics Lab, NASA Goddard Space Flight Center,*
*8800 Greenbelt Road, Greenbelt, MD 20771 USA*

[36] *VU University Amsterdam, 1081 HV Amsterdam, The Netherlands*

[37] *Nikhef, Science Park 105, 1098 XG Amsterdam, The Netherlands*

[38] *Dipartimento di Fisica, Università di Trento and Trento Institute for*
*Fundamental Physics and Application, INFN, 38123 Povo, Trento, Italy*

# Abstract

Albert Einstein recognized that gravitational waves were predicted as a consequence of his 1915 Theory of General Relativity (GR), but he thought that the effect was so small as to be of no practical consequence [1]. The 100 years since the publication of his theory saw significant development of the understanding of the theory, the identification of potential astrophysical sources of sufficiently strong gravitational waves, and development of key technologies for gravitational-wave detectors. In 2015, the first signals were detected by the two US Advanced LIGO instruments; in 2017, Advanced LIGO and the European Advanced Virgo detectors pinpointed a binary neutron star coalescence that was also seen across the electromagnetic spectrum. The field of gravitational-wave astronomy is just starting, and this roadmap of future developments surveys the potential for growth in bandwidth and sensitivity of future gravitational-wave detectors and discusses the science anticipated to come from these new instruments.

## INTRODUCTION

The past five years have witnessed a revolution in astronomy. The direct detection of gravitational waves (GWs) emitted from binary black hole (BBH) merger GW150914 (Figure 1) by the Advanced Laser Interferometer Gravitational Wave Observatory (LIGO) detector [2] on September 14, 2015 [3] was a watershed event, not only in demonstrating that GWs could be directly detected but more fundamentally in revealing new insights into these exotic objects and the Universe itself. On August 17, 2017 the Advanced LIGO and Advanced Virgo [4] detectors jointly detected GW170817, the merger of a binary neutron star (BNS) system [5], an equally momentous event leading to the observation of electromagnetic (EM) radiation emitted across the entire spectrum through one of the most intense astronomical observing campaigns ever undertaken [6]. Coming nearly 100 years after Albert Einstein first predicted their existence but doubted that they could ever be measured, the first direct GW detections have undoubtedly opened a new window on the Universe. The scientific insights emerging from these detections have already revolutionized multiple domains of physics and astrophysics, yet they are 'the tip of the iceberg', representing only a small fraction of the future potential of GW astronomy. As is the case for the electromagnetic Universe, different classes of astrophysical sources emit GWs across a broad spectrum ranging over more than 20 orders of magnitude, and require rather different detectors for the range of frequencies of interest (Figure 2).

In this review, we present the perspectives of the Gravitational Wave International Committee (GWIC) [7] on the emerging field of GW astronomy and physics in the coming decades. GWIC was formed in 1997 to facilitate international collaboration and cooperation in the construction, operation and use of the major GW detection facilities world-wide. Among its primary goals are to promote international cooperation in all phases of construction and scientific exploitation of GW detectors, to coordinate and support long-range planning for new instruments or existing instrument upgrades, and to promote the development of GW detection as an astronomical tool, exploiting especially the potential for multi-messenger astrophysics. Our intention in this article is to present a survey of the science opportunities and to highlight the future detectors that will be needed to realize those opportunities. The recent remarkable discoveries in GW astronomy have spurred GWIC to reexamine and update the GWIC roadmap originally published a decade ago [8].

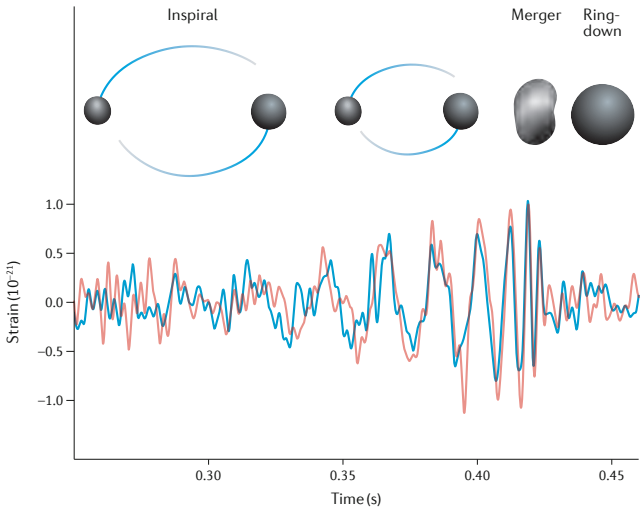


FIG. 1. The detected gravitational-wave strain amplitude as a function of time for GW150914, the first signal detected nearly simultaneously by the LIGO Hanford and Livingston Observatories. The waveforms are shifted and inverted to compensate for the slightly different arrival times and different orientations of the detectors (red: LIGO Hanford, blue: LIGO Livingston). The upper inset is a simulation of the merger produced using a numerical relativity simulation to illustrate the evolution of the black hole event horizons as system coalesces and merges.

In Section 2, we present an overview of GWs, the methods used to detect them, and some scientific highlights from the past five years. Section 3 provides a detailed survey of some of the outstanding scientific questions that can be answered with planned or envisioned future GW detectors. In section 4, we discuss the future prospects for synergistic observations using GW and electromagnetic observatories while in Section 5 we discuss the technological challenges to be overcome to build those detectors. We briefly summarize and present our conclusions in Section 6.

## GRAVITATIONAL WAVES: FUNDAMENTALS AND DETECTORS

Fundamentally different from and complementary to other astrophysical 'messengers' such as light, neutrinos, or cosmic rays, GWs provide unique information about the most energetic astrophysical processes in the Universe by carrying information about the dynamics of massive objects such as black holes and neutron stars moving at relativistic speeds. As

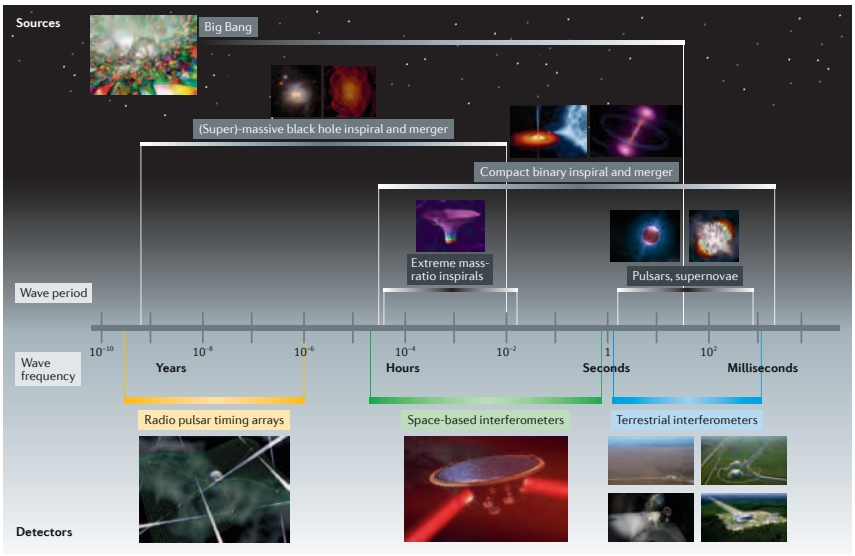


FIG. 2. The GW spectrum probed by strain sensitive GW detectors, ranging from $10^{-11}$ Hz to more than 1000 Hz. Source classes are shown above the spectrum; detectors are shown below. The portion of the GW spectrum below $10^{-11}$ probed through measurements of the cosmic microwave background polarization is not shown.

predicted by GR, GWs travel at the speed of light and possess two polarizations.

Gravitational waves physically manifest themselves as time-dependent strains, $h$, in space-time, or more precisely $h = \delta L/L$, where $L$ is the distance between two reference points in space and $\delta L$ is the induced displacement over the baseline $L$. The induced strain is perpendicular to the axis of GW propagation, and is quadrupolar, i.e., a wave traveling along the $z$ axis stretches (then compresses) the path along the $x$ axis while shrinking (then stretching) the $y$ axis (for one polarization; in the orthogonal polarization, the elongation/compression occurs along axes rotated 45 deg relative to the x- and y- axes). GW detectors rely on a measurement of variations in the light travel time between separated reference points – or 'test masses' – caused by a passing GW. The test masses are configured such that each is in near-perfect free-fall (and as such approximate a local inertial frame), and are separated over very long baselines. The light travel times between pairs of test masses are monitored and read out via a detector such that any changes in the space-time curvature caused by passing GWs induce modulations in these light travel times. This concept is simply illustrated for ground-based detectors in Figure 3, which shows a simple Michelson interferometer.

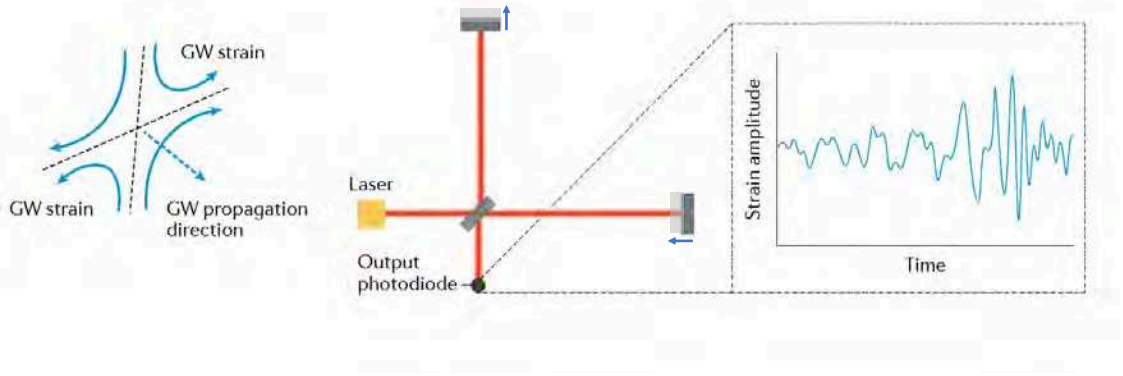


FIG. 3. A simple laser interferometer GW detector. A GW strain shortens one arm while lengthening the other as is passes the detector, resulting in a slight difference in round-trip travel time for the laser light. This in turn leads to a phase shift of the light in one arm of the detector relative to the other, creating a change in light intensity at the photodetector. The time-dependent intensity recorded by the photodetector produces a reconstruction of the propagating GW.

### Ground-based Detectors

Current ground-based observatories probe the high-frequency portion of the GW spectrum from ∼10 Hz to ∼10 kHz dominated by stellar-mass compact sources such as coalescing BBH and neutron star systems, and (as yet to be observed) supernovae and isolated neutron stars. All ground-based detectors use enhanced Michelson interferometry with suspended mirrors to directly measure a GW's phase and amplitude. The detection of audio-band GWs places extremely stringent demands on the isolation of the mirrors from local forces and disturbances. The two US-based Advanced LIGO detectors [2] have $L = 4$ km arm lengths, while the European-based Advanced Virgo [4] has $L = 3$ km arms. Typical strains from astrophysical sources are on the order of $10^{-21}$ or less, thus displacement sensitivities $\delta L$ of less than $\sim 10^{-18}$ m are required to detect GWs with sufficient signal-to-noise (SNR) ratio. (This is an incredibly small displacement; for comparative purposes note that the radius of a proton is $\sim 8.5 \times 10^{-16}$ m.)

Figure 4 shows a schematic view of Advanced LIGO, which serves to illustrate the configuration of the current generation of ground-based detectors. The mirrors are suspended from multi-stage pendulum systems such that, above the resonant frequencies of the suspension system (typically around 1 Hz), they can be effectively treated as in free fall (i.e., in a local intertial frame) in the light propagation direction. These suspensions and accompanying seismic isolation systems reduce the undesired test-mass motion induced by ambient ground motion by about a factor of $10^{12}$ from 1 Hz to 10 Hz [4, 9]. Beyond this, there are three primary noise sources that currently limit interferometer sensitivity: thermal noise produced by random displacements of the mirror surfaces that are produced by thermally fluctuating stresses in the mirror coatings, substrates, and suspensions [10]; Newtonian (or dynamic gravity gradient) noise arising from earth (ground) and atmospheric density perturbations directly exerting dynamic forces on the mirrors [11]; and quantum noise resulting from both vacuum fluctuations of the electromagnetic field that limit phase resolution in the readout photodetector (so-called 'shot noise') and displacements of the mirrors via quantum radiation pressure noise (QRPN) which induce stochastic impulses (or 'kicks') on the mirrors due to the random arrival time of the photons [12]. The effect of QRPN is diminished as the mirror mass increases, and both QRPN and shot noise can be reduced by injecting quantum-engineered squeezed vacuum states of light into the interferometer [13]. Thermal noise manifests itself in a variety of ways in mirror coatings, mirror substrates, and suspensions [14]; it can be understood from a statistical mechanics perspective as infinitesimal internal motions of macroscopic objects at non-zero temperatures caused by intrinsic dissipation (or mechanical loss) in the system. In addition to these fundamental noise sources, a very large number of technical noises must be identified and overcome, which broadly group into laser frequency and intensity noises, acoustically and seismically driven scattered light noises, sensor and actuator noises, stochastic forces from electrical and magnetic fields, and potentially energy deposited by energetic particles.(More details about these noise sources are presented in Section 5 where we discuss some of the challenges to building future ground-based detectors.)

To deliver the best science, a network of globally distributed interferometers functioning as a unified detector is required. The Advanced LIGO and Advanced Virgo detectors have actively searched the GW sky in a highly coordinated campaign during a series of observing runs carried out beginning in 2015. The detectors have achieved sensitivities sufficient to

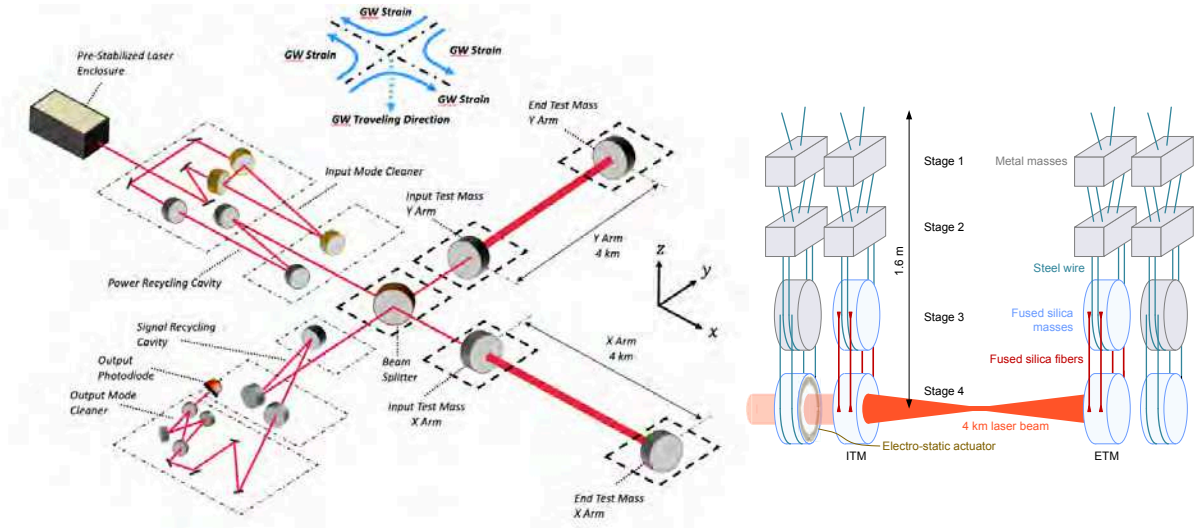


FIG. 4. (*Left*)A simplified view of the Advanced LIGO interferometer, showing the optical configuration including the laser, input mode cleaner, power- and signal-recycling cavities, the 4 km long arm cavities, and the output mode cleaner. The GW signal is recorded on the output photodiode after the output mode cleaner. (*Right*) A schematic of one of the arm cavities. The mirrors are held by quadruple suspensions to suppress ground motion disturbances.

detect BBH mergers on a weekly basis in their latest observing run [15]. The KAGRA detector [16, 17], a 3 km arm length interferometer in located underground in Japan, recently joined LIGO and Virgo to form the LIGO-Virgo-KAGRA network; the LIGO-India [18] interferometer will be joining later in this decade, dramatically improving the ability of the network to confidently detect and locate GW events [19] and providing new methods for testing alternative theories of gravity through enhanced ability to resolve GW polarizations [20].

The LIGO-Virgo observations have in a few short years already produced significant revelations about some of the most energetic and cataclysmic processes in the Universe. From GW150914, and more recent BBH mergers observed by the LIGO Scientific and Virgo Collaborations, we now know that there is a population of black holes paired in orbitally bound binary systems that evolve through the emission of GWs and merge in less than a Hubble time (the age of the Universe); that black holes of many tens and even hundreds

of solar masses exist in nature; and that the properties of the observed black holes are entirely consistent with GR to within current measurement limits [15, 21–29]. The BNS detection GW170817 and subsequent observations in the electromagnetic domain collectively comprise the first demonstration of GW-EM multi-messenger astronomy, providing an astounding wealth of knowledge including the first definitive link between binary neutron star merger progenitors and short gamma ray bursts [30–33], the first definitive observation of a kilonova [34–43], conclusive spectroscopic proof that BNS mergers produce heavy elements through $r$-process nucleosynthesis [44–49], the first demonstration that GWs travel at the same speed as light to better than a few parts in $10^{15}$ [30], and an independent method for measuring the Hubble constant using detected GWs as a "standard siren" for determining the absolute distance to the source [50**?** , 51]. Additionally, the Advanced LIGO and Advanced Virgo detections have enabled tests of GR in the strong gravity regime that were inaccessible to other experiments and astronomical observations [52, 53], motivating research on many fronts in fundamental physics and astrophysics. We emphasize that this represents a very brief overview of the recent discoveries and, as we discuss in detail below, captures only a fraction of the potential science afforded by future GW observations.

**Space-based Detectors**

When launched in the mid-2030's, the Laser Interferometer Space Antenna (LISA) [54] will possess a breathtaking scientific portfolio. LISA will explore much of the GW Universe in the frequency band from 100 $\mu$Hz to 100 mHz. A constellation of three satellites separated by $2.5 \times 10^9$ m in a trailing earth orbit, LISA will be capable of detecting the first seed black holes formed out to $z \sim 20$ or more [55], and discover intermediate-mass and 'light' super-massive coalescing black hole systems in the $10^4$–$10^7$ solar mass range, thus tracing the evolution of black holes from the early Universe through the peak of the star formation era. Through detections of extreme mass ratio inspirals (EMRIs, binary systems with mass ratios as small as $\sim 10^{-6}$) [56], LISA will directly map the curvature of space-time at the event horizons of massive black holes, yielding even more precise tests of GR in the strong gravitational field regime. LISA might also detect stellar-mass BBH systems years before they are detectable by ground-based detectors [57], and provide very precise sky localization of such events for electromagnetic follow-up. By discovering new sources of Galactic compact

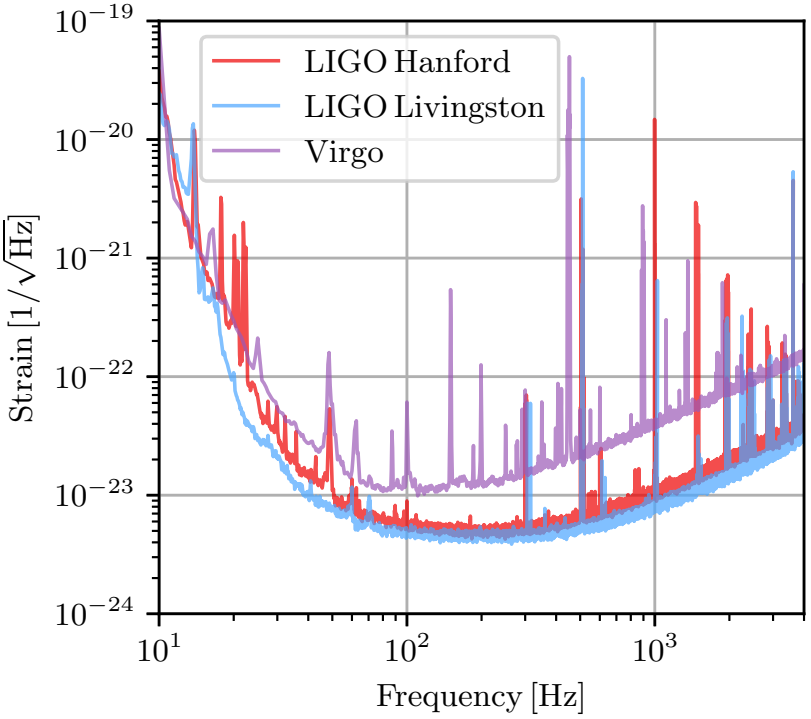


FIG. 5. The sensitivity of the LIGO-Virgo network for the latest 'O3' observing run plotted as a function of frequency. The vertical presents the sensitivity as an amplitude spectral density, i.e., the strain per unit square root of frequency. The stable narrow spectral features are due to very high-$Q$ mechanical resonances and electrical (50 or 60 Hz) coupling. At low frequencies, scattered light, seismic, and control noise dominate; in the mid-band, thermal noise in the mirror dielectric coatings is the leading term. At high frequencies, quantum noise is the limit to sensitivity.

binaries comprised of white dwarfs, neutron stars, and stellar mass black holes, LISA will survey the predominant population of binary compact objects and map the structure of the Milky Way [58].

The LISA Pathfinder (LPF) [59] launched in 2015 has paved much of the way for the full–scale LISA mission. LPF was a European Space Agency (ESA) mission, with contributions from a Consortium of European national agencies as well as NASA. It has already convincingly demonstrated some of the key performance requirements for the full LISA mission, most notably the displacement sensitivity and control of spurious acceleration noise required for LISA. More on LISA science is presented in Section 3, while LISA and LPF detector technology is discussed in detail in Section 4.

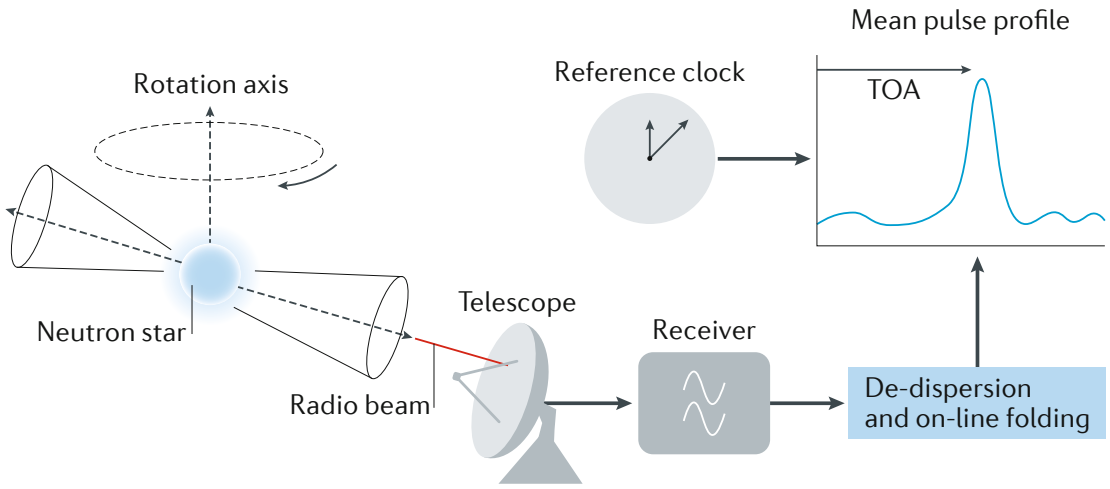


FIG. 6. Illustration of the radio pulsar timing process. The pulsar beams sweep across the radio antenna and are detected using a radio receiver at ∼GHz frequencies. The data are corrected for delays due to the interstellar medium ("dedispersion") and then folded at the period of the pulsar to create an integrated profile. This profile is then cross-correlated with a noise-free template profile to calculate a time of arrival (TOA), use a high-precision reference clock at the observatory.

**Pulsar Timing Arrays**

Pulsar timing arrays (PTAs) [60–63] explore the nanohertz portion of the GW spectrum ranging from $10^{-9}$ to $10^{-6}$ Hz. Rather than using laser light to measure variations in detector length as ground- and space-based detectors do, a PTA measures variations in the radiofrequency pulse arrival times at the earth from an array of millisecond pulsars [64, 65].

Figure 6 illustrates the pulsar timing process. Pulsars are rotating neutron stars that act like cosmic lighthouses, appearing as periodic pulsating radio sources. Because millisecond pulsars (MSPs), pulsars with periods between roughly 1.4 and 30 ms, possess rotational stabilities comparable to the best atomic clocks, they are ideal timing sources. Once effects such as rotational spin-down, astrometric position and motion, and orbital effects from binary companions are accounted for, the pulse arrival times can be precisely modeled and predicted to fractions of a microsecond for up to decades into the future [66], and variations arising from GW perturbations can be measured. Distortions in the spacetime around earth

or the pulsars will produce systematics in timing residuals (deviations of the measured pulse arrival times relative the predicted arrival times), and crucially, spatially correlated systematics in the timing residuals of the array of pulsars across the sky [67]. A GW emitted from a single binary system passing the pulsar-earth system will cause two frequency components in the time-series of the timing residuals: one from the spacetime variations at the pulsar ("pulsar term"), the other from variations at the earth ("earth term"), with different frequencies resulting from changes in the orbital frequency of the emitting source during the time it takes for the radio pulses to travel to the earth. The top panel of Figure 7 shows the expected detection in the form of the Hellings-Downs curve, the correlated response of a pair of pulsar-earth baselines to a stochastic GW background averaged over all sky positions and polarizations as a function of angle between the pulsar pair-earth baselines [67].

Pulsars are observed at monthly or more rapid cadences in order to sample and measure changing properties such as the position of the pulsar (i.e. proper motion) and varying dispersion due to the interstellar medium. In addition, they must be observed for roughly one half-hour per observation to average over enough of the noise-like pulses to mitigate the effects of pulse jitter. The observations themselves cover very wide bandwidths (>GHz) or occur near-simultaneously at multiple radio frequencies in order to correct for the effects of interstellar dispersion. Pulsar timing instruments must have fine frequency resolution ($\sim$1 MHz) to correct for these effects, coupled with high time resolution in order to sufficiently sample the roughly millisecond wide radio pulses.

As each pulsar needs to be timed for about a year (i.e. one earth orbit) to be properly localized and understood, PTA experiments must have years-long durations. In practice, the lower end of the frequency window is given by the length of the data set (i.e. currently about 1 nHz), while the upper end is given by the cadence of the timing observations (i.e. currently about 1 $\mu$Hz). Timing residual amplitudes of about 100 ns or less are resolved for the best timed millisecond pulsars.

Today there are three major pulsar timing arrays: the Parkes PTA [68] in Australia, the European PTA consortium [69], and the NANOGrav [70] consortium in North America. These arrays regularly achieve sub-microsecond timing on over 100 millisecond pulsars (MSPs) which collectively form the International Pulsar Timing Array [71] (IPTA). PTA science is often sensitivity-limited, and many of the MSPs being discovered in recent surveys have flux densities that often require hour-long observations with 100-m class (or larger) tele-

scopes to achieve the requisite sub-microsecond timing. Recently however, the FAST (500 m diameter) and MeerKAT (64 antennas, $\times$ 13.7 m diameter) telescopes have been commissioned, and are now commencing regular MSP timing, joining many existing 64–100 m class facilities in the Northern hemisphere, and the Parkes 64 m telescope in the Southern hemisphere. Figure 7 illustrates the radio telescopes used for pulsar timing experiments around the globe.

The most promising GW sources in the nanoHertz band are super-massive ($10^7 - 10^{10}$ $M_\odot$) binary black holes (SMBBHs) that form via the collisions of massive galaxies. The Astrophysical Stochastic GW Background (ASGWB) produced by the cosmic population of slowly inspiralling SMBBHs across the Universe [72–74] is the first signal likely to be detected, followed by individual SMBBH [75–77]. The detection of an ASGWB will reveal essential information about the formation of the large-scale structure of the Universe, determine the rates of galaxy mergers, and definitively resolve the "final parsec" problem [78] – the theoretical difficulty of shrinking the orbit of a SMBBH by a factor of $\sim$100 after its formation at a separation of $\sim$1 pc via scattering of stars. PTA measurements are currently probing the expected range of astrophysical signals [79–82], and based on recent results a detection of the ASGWB is likely imminent [74]. Detection of individual SMBBHs will allow for combined electromagnetic and GW multi-messenger observations and, though only a handful are expected, the scientific return of these discoveries will be immense [83].

**Cosmic Microwave Background Polarization**

The lowest frequencies of the GW spectrum, down to approximately $10^{-18}$ Hz, are populated by a stochastic background of remnant primordial GWs produced during the Big Bang. Standard inflationary cosmology predicts a GW spectrum too feeble to be detectable by current ground-based detectors, LISA, or PTAs, although some extensions of inflation and more exotic models, including first order phase transitions and topological defects, predict primordial GW energy densities that can be detected across the frequency bands [84, 85]. Electromagnetic-based measurements of the Cosmic Microwave Background (CMB) polarization may reveal signs of the remnant primordial GWs [86]. As CMB polarization measurements are based on a fundamentally different detection method than their higher frequency counterparts, this approach is not discussed further here.

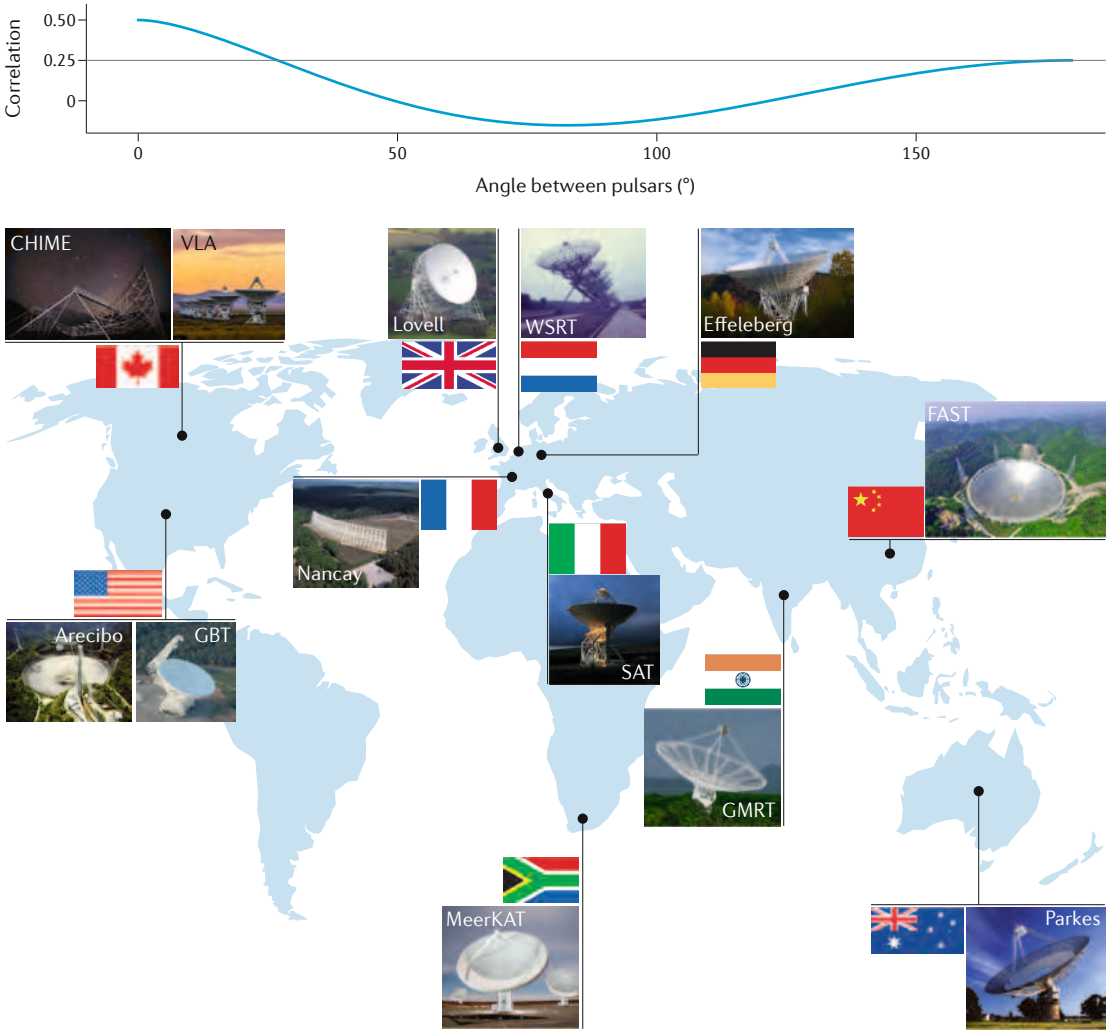


FIG. 7. *Top:* The "Hellings and Downs curve" showing the correlation in pulsar timing residuals as a function of MSP angular separation that we expect to detect. *Bottom:* The telescopes that will be used for this experiment. Arecibo (Puerto Rico), the Green Bank Telescope (GBT; West Virginia), Lovell (U.K.), Effelsberg (Germany), Nançay(France), Westerbork Synthesis Radio Telescope (WSRT; Netherlands), Sardinia Radio Telescope (SRT; Italy), and Parkes (Australia) are currently contributing IPTA data. The Very Large Array (VLA; New Mexico) will soon begin to contribute. The Deep Space Station-43 (DSS-43; Australia), the Molonglo Observatory Synthesis Telescope (MOST; Australia), the Giant Meterwave Radio Telescope (GMRT; India) and Ooty (India) as well as three under-construction telescopes – CHIME (Canada), Five hundred meter Aperture Spherical Telescope (FAST; China), and MeerKAT (South Africa).

## PURSUING ASTRONOMY AND PHYSICS WITH GRAVITATIONAL WAVES IN THE COMING DECADES

In the coming decades, the new observational window of GW astronomy promises to deliver data that will transform the landscape of physics, addressing some of the most pressing problems in fundamental physics, astrophysics, and cosmology [83, 87–90]. The next generation of ground-based GW observatories planned for the 2030s, the Einstein Telescope (ET, [91]) and Cosmic Explorer (CE, [92]) (collectively referred to as 3G), as well as the LISA [54] mission, will observe merging black holes and neutron stars when the Universe was still in its infancy. Pulsar Timing Networks (PTA[71]) will continue to evolve to greater sensitivity. LIGO Voyager [93], a major upgrade under consideration for the current LIGO observatories late this decade, could test some of the key technologies needed for the ET and CE and at the same time provide a significant increase in sensitivity over the current generation of detectors. With all of these instruments we can expect to witness extremely high SNR events that could reveal subtle signatures of new physics. The revolutionary potential of GW science in the next two decades is typified by Figure 8, which compares the reach of the current ground-based detectors Advanced LIGO and Advanced Virgo with that of planned 3G observatories for 1.4 – 1.4 $M_\odot$ BNS and 30 – 30 $M_\odot$ BBH mergers as a function of redshift and 'look back' time toward the Big Bang.

### Fundamental Physics

Gravitational-wave observations, because they can explore the most extreme conditions of spacetime and of matter, can serve as unsurpassed probes of fundamental physics. In this section we will look at the power of this new tool in exploring gravity and matter at their most extremes.

*Testing GR and modified theories of gravity* GR has been a tremendously successful theory in explaining current astronomical observations and laboratory experiments [94–96]. Nevertheless, there is a general consensus that GR is at best incomplete, representing an approximation to a more complete theory that cures some or all of its problems [97]. Theoretical difficulties include loss of information down a black hole [98], which contradicts unitary evolution of physical states in quantum mechanics; inevitability of spacetime singu-

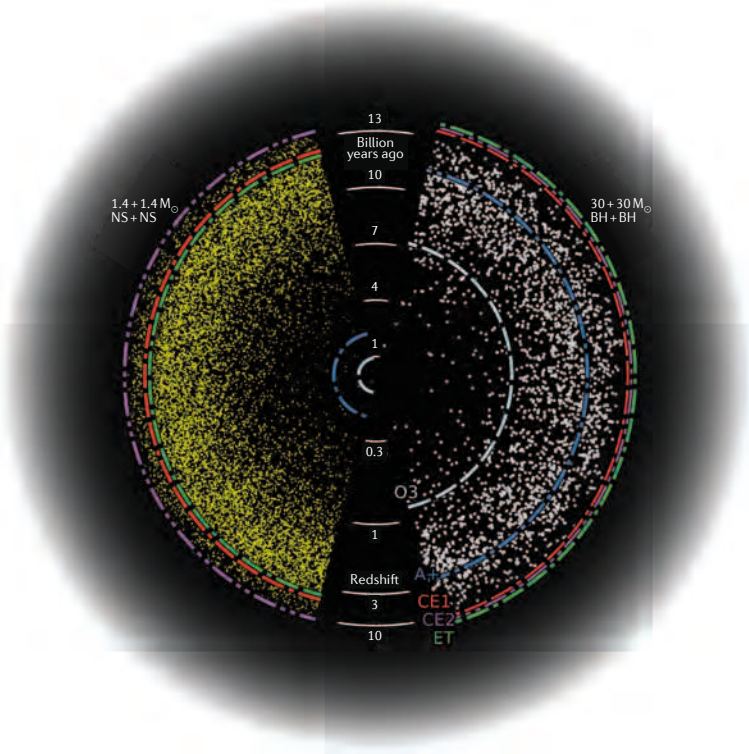


FIG. 8. The conceptual reach of next-generation ground-based detectors showing the range of the current ground-based detectors and future planned detectors Einstein Telescope and Cosmic Explorer to detect 1.4-1.4 solar mass BNS (left) and 30-30 solar mass BBH (right) mergers as a function of 'look back' time (to the Big Bang) and redshift. CE is envisioned to be implemented in two phases, designated CE1 and CE2. At their ultimate planned sensivities, ET and CE will be able to observe all stellar mass BNS and BBH mergers.

larities [99, 100], for example at the centre of a black hole where physical quantities such as the density and curvature of spacetime become infinitely large; a cosmological constant that is responsible for the late-time accelerated expansion of the Universe [101, 102], whose value cannot be accounted for in the Standard Model of particle physics [103]; and the lack of a viable formulation of quantum gravity, which might resolve all of these problems but has so far been elusive. These difficulties have increased interest in searching for GR violations in observations with the hope that they will provide clues to an alternative theory of gravity.

From an observational point of view, the past few decades have witnessed a series of compounding problems in cosmology that simply won't go away, including the accelerated

expansion of the Universe [101, 102], tension between the local and early Universe measurements of the Hubble constant [104], and lack of direct observation of dark matter [105]. As we discuss below, these are each prime examples of outstanding puzzles in modern physics where observations of GWs may enable progress.

The spacetime curvature at the horizon of a black hole of mass $M$ and radius $R \sim 2GM/c^2$ goes as $\kappa \sim \sqrt{GM/c^2R^3} = c^2/\sqrt{8}GM$. Note that $\kappa$ is larger for lighter black holes, thus binary coalescences of lightest astrophysical black holes are, therefore, the strongest regions of gravity that we know of and are ideal for testing strong field predictions of GR [96, 97]. Sub-solar mass black hole binaries, should they exist, would have even greater curvature. Although neutron stars are lighter than astrophysical black holes they are not as compact and hence probe smaller curvature scales. Black hole mergers also probe regions of greatest compactness (or dimensionless gravitational potential) defined as $\Phi = GM/c^2R$, which is largest for black holes. Past experiments such as the double pulsar orbital decay [106] or the Cassini spacecraft [107] confirmed GR in moderately strong fields (see Fig.9). Current and future experiments such as the Event Horizon Telescope (EHT) [108] and the GRAVITY instrument [109] explore the spacetime of massive black holes and hence small curvature and high compactness. X-ray observations by the NICER experiment [110] will probe GR in the high curvature and compactness of neutron stars [111] while GW observations of stellar-mass black holes by ground-based detectors ("GW ground" in Fig. 9) and LISA probe regions of greatest curvature and compactness on a wide range of scales: stellar-mass black holes of up to $\sim 100M_\odot$ (mostly ground-based observatories but also LISA for sources that are close by), intermediate mass black holes of $10^2$–$10^4\,M_\odot$ (ground-based observatories and LISA) and super-massive black holes of $10^5$–$10^{10}\,M_\odot$ (LISA at the lower end and PTAs at the higher end of the mass range), offering tests of GR over ten orders of magnitude in length scale and twenty orders of magnitude in curvature.

In addition to probing the strong field predictions of GR, the vast cosmological distances over which gravitational waves travel (redshifts in excess of $z \sim 20$ both in the case of LISA and ground-based detectors) will greatly constrain local Lorentz invariance and graviton mass [94]. Violations of Lorentz invariance or a non-zero graviton mass could cause dispersion in the observed waves and hence help to discover new physics predicted by certain quantum gravity theories. At the same time, propagation effects could also reveal the presence of large extra spatial dimensions that lead to different values for the luminosity distance

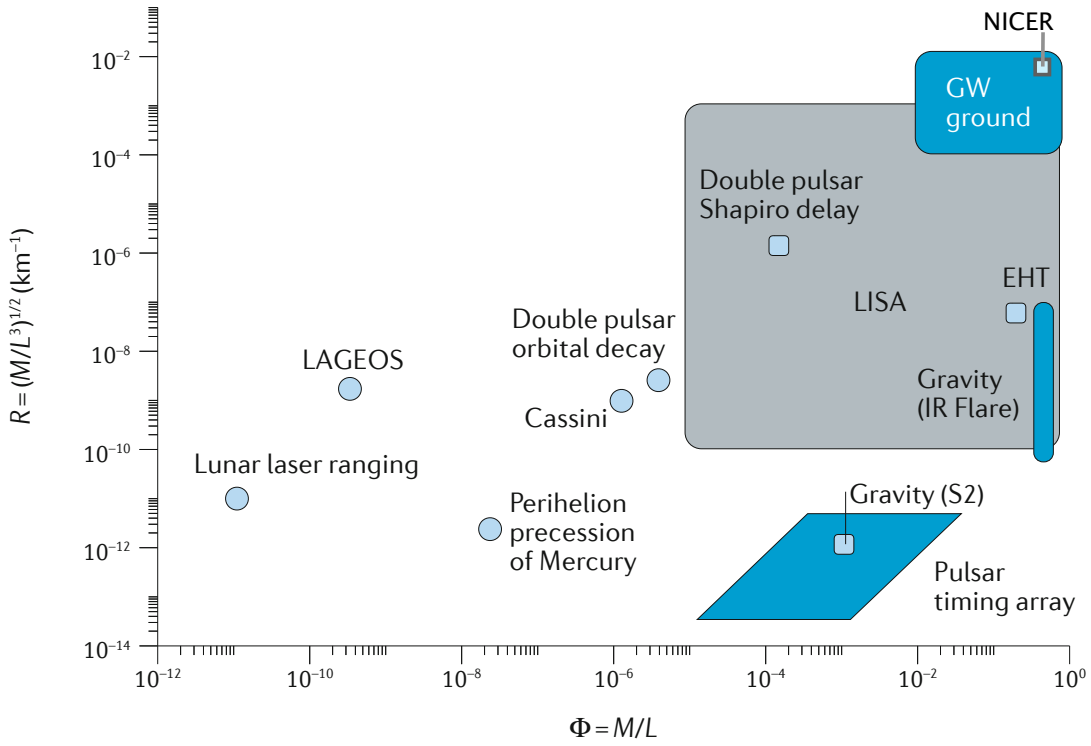


FIG. 9. Gravitational-wave observations offer a unique ability to test GR in regions of high curvature and strong gravity. The plot shows the curvature scale $\kappa$ (in km$^{-1}$) due to the presence of mass $M$ of size $R$ defined as $\kappa \equiv \sqrt{GM/c^2R^3}$ and the compactness, or the dimensionless gravitational potential, $\Phi \equiv GM/c^2R$ probed by different experiments. For example, observation of the double binary pulsar (total mass of 2.6 $M_\odot$ and orbital separation of $\sim 10^6$ km) probes the curvature scale of $\kappa \sim 2 \times 10^{-9}\,\mathrm{km}^{-1}$ and compactness of $\Phi \sim 4 \times 10^{-6}$. In contrast a black hole binary of total mass 10 $M_\odot$ at the time of merger probes a curvature scale of $\kappa \sim 2.4 \times 10^{-2}\,\mathrm{km}^{-1}$ and compactness of $\Phi \sim 0.5$. Filled circles represent past experiments that have verified GR at the corresponding curvature scale and compactness. Rectangles and rhombus represent ongoing or future experiments that will probe ever greater scales of curvature and compactness.

to a source inferred by GW and electromagnetic observations (see, e.g. [112, 113]) or cause birefringence of the waves predicted in certain formulations of string theory as discussed in Ref. [114, 115]. In certain modified gravity theories GWs have more than two polarizations (in contradiction with GR); the presence of such additional degrees of freedom could be explored by future detector networks [94, 116].

*Equation of state of ultra-high density matter* Neutron star cores can reach densities many times that of nuclear saturation density ($\sim 2 \times 10^{17}\,\mathrm{kg\,m^{-3}}$), making them the regions of the highest matter density known in the Universe [117]. With colliding binary neutron stars (and neutron star-black hole binaries) we can probe the structure of cold, ultra-high density matter [118]. Some fifty years after pulsars were first discovered [119], we still do not have a good understanding of the physics of neutron stars, especially the composition of their inner core. It is possible that the core is simply a gigantic nucleus or a sea of free quarks and gluons. Nucleons in neutron star cores could undergo a phase transition to quark-gluon plasma [120, 121] at the super-high densities that might be found in the hypermassive neutron stars [122, 123] that form in the aftermath of the merger of two neutron stars and live briefly before collapsing to a black hole. Gravitational waves emitted during the last few cycles of inspiral of neutron stars and the ringdown of the remnant carry the crucial signatures of the properties of their cores and hot dense matter equation of state.

A neutron star in a binary system can tidally deform its companion, which can cause the system to inspiral and merge more rapidly [124]. The tidal deformation is greater for neutron stars with larger radii or cores with stiffer equations-of-state as in the case of hadronic matter. Conversely, cores comprised of unbounded quark matter will have smaller radii and be harder to deform; thus tidal effects wouldn't alter the orbital evolution as much. The tidal effects are directly encoded in the emitted GWs but the effect arises at fifth-post-Newtonian order (or at $\mathcal{O}(v/c)^{10}$ in post-Newtonian expansion) [124]. Moreover, the post-merger phase could also see GW emission from the (initially) highly deformed hypermassive neutron star [125]; the spectral features of the emitted signal can be mapped directly to the equation of state of 'hot' dense matter, including possible phase transitions [126–128].

GW170817 ruled out some of the stiffest equations of state and determined the radii of companions to be in the range from 9–13 km [5, 6]. Third generation ground-based observatories will constrain the radius to within a few hundred meters and help measure central densities and pressures in neutron stars. They will also detect post-merger waveforms and provide constraints for 'hot' equations of state [126–128] and possibly offer clues of quark deconfining phase transitions [120, 121].

*Exploring dark matter properties with GW observations* Black hole and neutron star mergers could provide unique insight into nature of dark matter [129], another long-standing problem in astrophysics and cosmology. Much of what we know about dark matter comes

from its gravitational influence on the dynamics of stars and galaxies and the cosmic microwave background. Dark matter, in extensions of the Standard Model, is conceived to be comprised of weakly interacting massive particles (WIMPS) [130] or possibly extremely light particles such as axions that were proposed to solve the strong CP problem in quantum chromodynamics [131].

Efforts are underway to make a direct detection of WIMP and axionic dark matter in laboratory experiments, however these experiments have not been successful to date. Gravitational wave observations could help infer the properties of dark matter in several ways although any inference drawn will still be indirect evidence of their properties. For example, in the presence of dark matter fluid, BBHs would experience a drag force that would alter their general relativistic orbital dynamics. This signature could be extracted from the frequency evolution of the observed GW [132].

Dark matter could be composed, at least in part, of ultralight bosons such as QCD axions [133], dark photons or other light particles [134], spanning a wide mass range of $10^{-33}\,\mathrm{eV}$–$10^{-10}\,\mathrm{eV}$ [133, 134]. The Compton wavelength of ultralight bosons in the mass range $10^{-20}\,\mathrm{eV}$–$10^{-10}\,\mathrm{eV}$ corresponds to the horizon size of black holes of mass $10\,M_{\odot}$–$10^{10}\,\mathrm{M}_{\odot}$. Although these ultralight fields may not interact with other Standard Model particles, the equivalence principle implies that their gravitational interaction with, e.g. black holes, could have observable consequences. For example, bosonic fields whose Compton wavelength matches the horizon scale of an astrophysical black hole could form bound states (often called 'gravitational atoms') around black holes and extract their rotational energy and angular momentum via the mechanism of superradiance [135, 136]. This would result in a Bose-Einstein condensate that acts as a source of continuously emitted GWs. Ground-based detectors would explore the higher end of the mass range from $10^{-13}\,\mathrm{eV}$ to $10^{-10}\,\mathrm{eV}$, which correspond to QCD axions. LISA could explore the presence of even lighter bosonic fields.

Primordial black holes have also been proposed to constitute dark matter and gained attention after LIGO's first discovery of stellar black holes with unusually large masses [137].

**Cosmology**

Gravitational-wave observations have the potential to make fundamental contributions to cosmology. Much of this science arises from the fact that merging binary systems are "standard sirens", that is, the signal contains direct information about the luminosity distance to the source [50, 138]. This information can be extracted from the signal provided the detector network can localize the sky position of the source and measure the polarization of the signal.

*Hubble constant* LIGO and Virgo with EM observers made their first measurement of the Hubble constant using the standard siren GW170817 [51], and it continues to be refined [139]. Stand-alone measurements are also possible via a statistical association between a GW source and nearby galaxies [140]. The current ground-based network, recently augmented by KAGRA and later this decade by LIGO-India, is expected to improve this to a precision of a few percent. These measurements do not rely on astronomical distance ladders, so they provide an important check on systematic errors and other assumptions used in other methods. They may help resolve the existing tension between the two principal Hubble constant measurement methods [141, 142], clarifying if this is due to measurement issues or new physics.

*Dark energy* Big Bang cosmology is largely consistent with GR; however, the accelerated expansion of the Universe in its recent history cannot be explained by the theory, indicating either its failure in that our cosmological principles are too simple or there exists an exotic form of matter-energy density termed *dark energy* [143]. Many dedicated telescopes are being built to try to ascertain the nature of dark energy. GW observations offer an independent tool for understanding the acceleration and the nature of dark energy, via the ability of binary neutron stars and black holes to serve as GW "standard sirens". LISA and 3G detectors will reach to higher redshifts, enabling them to measure the amount of dark energy and possibly the dark energy equation of state, even without counterpart identifications. The large population of BNS mergers out to $z = 2$ or more that is expected to be detected by the 3G network will allow a test of cosmological isotropy: do the distances to these events vary around the sky in a statistically significant way? On smaller angular scales, these distances will also allow independent estimates of weak lensing, mapping the dark matter. The large variety of sources observed by LISA will provide different classes of standard sirens. Stellar

black hole binaries at $z \lesssim 0.2$ (Ref. [144]), EMRIs at $z \lesssim 1$ (Ref. [145])and SMBBHs up to $z \approx 10$ (Ref. [146]) will enable precision cosmology across the whole astrophysically relevant redshift range.

Gravitational-wave observations can also aid in inferring the equation of state of dark energy. With a population of compact binary mergers observed with 3G detectors, and their redshifts obtained by follow-up electromagnetic observations, it will be possible to accurately measure cosmological parameters such as the dark matter and dark energy densities and the equation of state of dark energy, giving a completely independent and complementary measurement of the dynamics of the Universe.

*Astrophysical and primordial stochastic backgrounds* The ASGWB that will be detected by PTAs also contains cosmological information. The properties of the ASGWB depend on the formation and evolution of cosmological source populations [81]. PTA measurements of the ASGWB produced by SMBBHs, the most promising GW source in that band, will constrain the evolution of the super-massive black holes that become quasi-stellar objects (QSOs) and active galactic nuclei (AGNs). In addition, PTAs are sensitive to GWs produced by fundamental physical phenomena such as phase transitions in the early Universe, cosmic strings, and inflation, all of which would provide unique windows into high-energy and early-Universe physics [147, 148]. Finally, just as for ground- and spaced-based detectors, EM counterparts to individual SMBBH systems will allow for new measurements of the Hubble constant.

**Gravitational-Wave Astrophysics**

*Formation and evolution of compact stars* Binaries formed from pairs of compact stellar remnant objects such as white dwarfs, neutron stars, or black holes are efficient emitters of GWs. As these binaries form through various channels and enter the GW-driven regime of their evolution, they sweep up in frequency through first the mHz band of space-based detectors and eventually into the Hz to kHz band of ground-based interferometers [149]. Among those, the more massive systems (such as GW150914) will first sweep through the LISA band, crossing to the ground-based frequency band a few years later. LISA will allow precise determination of the sky location and time of coalescence weeks in advance, making it possible to schedule massive and deep EM coverage of the sky at the time of

merger. Such measurements can yield clues as to the likely progenitor systems and their evolution, providing an important constraint on models of stellar evolution. Detailed measurements of GWs from individual systems can also provide information about the internal structure of the objects involved, such as (discussed above) the equation of state of neutron stars involved in a neutron star-neutron star binary. Through interleaved operation and improvement of ground-based detectors, an ever larger statistical sample of BH-BH, neutron star-neutron star, and neutron star-black hole binary coalescences will be observed, enabling reconstruction of the formation and evolution of these systems along the cosmic history.

With the arrival of LISA in the 2030s, tens of thousands of BH and BNS binary systems will be added to the catalog [150]. The population of white dwarf-white dwarf binaries in the Milky Way will also be unveiled, enabling a range of astrophysical investigations: from the structure of our own galaxy, to the connection between white dwarf-white dwarf binaries and type Ia supernovae. Beyond the Milky Way, hundreds of stellar-mass BH binaries far from coalescence will be added to the event count, thus providing precious complementary information to that gathered by ground-based detectors.

*Super-Massive Black Hole Growth and Evolution* Super-massive black holes (SMBHs) having masses in the range from $10^6$–$10^{10}$ solar masses and inhabiting the centers of galaxies also frequently form binaries by pairing with other compact objects [151]. This may happen in the aftermath of a galaxy-galaxy merger, when two SMBHs pair with each other, resulting in the formation of an SMBBH; or as a result of dynamical processes in dense stellar nuclei, in which the capture of a stellar remnant (BH, NS or white dwarf) by a SMBH initiates an EMRI [152]. Both classes of sources are of capital importance in piecing together the puzzle of cosmic structure formation. We know today that virtually every massive galaxy hosts a SMBH at its center, that galaxies merge frequently, that proto-galaxies were already in place at $z > 10$, and that quasars were already shining at $z > 7$. These pieces of evidence led to the framework of hierarchical structure formation, whereby galaxies grow by accreting gas cooling along the filaments of the cosmic web and by merging with other galaxies. LISA has the capability to detect mergers of black holes in the mass range $10^3$–$10^7$ $M_\odot$ out to their formation redshift, including for $z > 20$ for some mass ranges [153]. Only GW detectors can observe individual objects at such early times. SMBBH mergers trace the assembly of their hosts from the formation of the first proto-galaxies following the dark ages, well beyond the epoch of re-ionization, up to now. By inferring the redshifts of these events from their

luminosity distances, LISA can follow the evolution of large-scale structure over time and, by exploring the demographics of black hole seeds (including their masses and spins), LISA can test models of how early black holes grow into the massive and SMBHs we see today in galaxies and quasars.

This information is complemented on the one hand by the observation of EMRIs up to $z \approx 1$, and on the other hand by the PTA detection [154] of the stochastic GW background produced by the most massive black hole binaries in the Universe. EMRIs can probe the population of inactive (thus otherwise invisible) SMBHs, providing invaluable insights into the low mass end of the SMBH mass function down to the mass scales of dwarf galaxies. The properties of individual inspirals (such as eccentricity and orbital inclination) carry information on the dynamical processes governing the evolution of dense relativistic systems, offering a unique laboratory for testing strong gravity.

At the super-massive end of the mass spectrum PTAs are expected to reveal the cosmic population of inspiralling SMBBHs that inhabit the largest galaxies in the Universe [77, 154]. These objects are in a frequency range inaccessible to LISA and ground-based detectors. Outstanding questions such as the precise occupation fraction of SMBHs in galaxies, the merger rate of galaxies, the relation between galaxy masses and the masses of the SMBHs they host, the efficiency of pairing of SMBHs, and the nature of their dynamical interaction with the environments at the cores of galaxies will be answered by deciphering the information encoded in the amplitude and shape of the ASGWB spectrum [83]. The detection of the ASGWB will definitively resolve the 'final parsec problem' proving that SMBHs can merge and possibly elucidating their dynamical interactions in the cores of galaxies. The dominant dynamical processes are expected to be scattering of stars on orbits that intersect the galactic core, or interactions with a circumbinary disk. PTAs probe frequencies at the interface between the environment-driven regimes (when the SMBHs are far apart) and GW-dominated regimes (when the SMBHs separations are below a milliparsec). Each dynamical mechanism also predicts different inspiral timescales compared with estimates that assume GW-driven inspiral, so measuring the ASGWB spectrum can provide clear evidence of which dynamical processes dominate in these massive galaxy hosts. Individual SMBBH systems are expected to be detected after the detection of the ASGWB. Studies of individual systems, coupled with EM observations, will allow us to probe the astrophysical processes driving mergers even further, and determine how the importance of various

processes depends on the properties of the galaxies [83].

## MULTI-MESSENGER ASTRONOMY WITH GRAVITATIONAL WAVES

*Dawn of a new multimessenger era* Detection of gravitational waves from the inspiral and merger of the first binary neutron star system GW170817 [5] marked the start of a era of multi-messenger astronomy incorporating GW observations [6]. The extensive multi-wavelength, multi-year follow-up campaign of GW170817 enabled the detection of counterparts in almost all the electromagnetic bands [6], confirming that the merger of a binary system of neutron stars powers high-energy transients, such as short gamma ray-burst [30, 155] and kilonovae [36, 156]. This unique multi-messenger detection [6, 35, 39] showed the potential of multi-messenger astronomy impacting our knowledge of relativistic astrophysics [42, 157], radioactively-powered transients [158], nucleosynthesis and heavy element enrichment of the Universe [44, 45], and the physics of dense nuclear matter [159–162]. It also showed the importance of population studies required to disentangle the micro-physics of the source and its interaction with the environment, from the source geometry and energetics [163]. Increasing the number of joint detections will make it possible to determine the equation of state of neutron stars [164], to probe the properties of different components of the mass ejected during and after the merger [165–167], to understand if the binary neutron-star mergers are the primary channel of formation of heavy elements and the details of the nuclear physics relevant to nucleosynthesis [168], and to understand the structure of the relativistic jets and the physics behind their formation [169].

*Multimessenger facilities* During this decade (2020–2030), the transient sky will be explored by new observatories and surveys, which will probe a range of frequency bands and time scales with better sensitivity than ever reached before. The better sensitivity will be crucial to follow-up GW signals coming from larger distances accessible by the upgrades of the LIGO, Virgo and KAGRA detectors, and the third generation of GW detectors. In the optical band, the Vera C. Rubin Observatory [170] will commence operation in early 2020s and serve as a unique resource for deep, multi-color searches for optical counterparts over hundreds of square degrees. The James Web Space Telescope (JWST) [171] and a new generation of 30 m–40 m class telescopes, such as the European Southern Observatory Extremely Large Telescope (E-ELT) [172], the Giant Magellan Telescope (GMT [173]) and

the Thirty Meter Telescope (TMT) [174], will allow us to characterize the nature of the GW source following the temporal evolution and spectral properties of the faint emission through deep imaging and spectroscopy. The high angular resolution and sensitivity of these telescopes will enable us to probe the local environment of the source, the properties of the host galaxy, and the possible presence of star clusters, giving us an insight to better understand formation and evolution of compact objects.

The high-energy sky is currently monitored by sensitive large field-of-view survey instruments, including NASA's Neil Gehrels Swift [175] and Fermi [176] satellites and European Space Agency's INTErnational Gamma-Ray Astrophysics Laboratory (INTEGRAL) satellite [177]. A number of future missions are envisioned, such as eROSITA [178], Einstein Probe [179], eXTP [180], the Space-based multi-band astronomical Variable Objects Monitor ECLAIRs (SVOM-ECLAIRs) [181], and the All-sky Medium Energy Gamma-ray Observatory (AMEGO) [182]. The sensitivity of the Advanced Telescope for High ENergy Astrophysics (ATHENA) X-ray observatory [183], which is expected to be launched around 2030, and the ambitious Lynx project [184], recently proposed in the US, will be necessary to detect fainter X-ray sources, such as the X-ray afterglow emission from relativistic jets observed off-axis. Mission concepts, such as the Transient High Energy Sky and Early Universe Surveyor (THESEUS [185]) and the Transient Astrophysics Probe (TAP [186]) are planned to have a unique combination of instruments for gamma-ray, X-ray and infrared transient detections to catch non-thermal and thermal emissions from GW sources.

In the radio band, the Square Kilometer Array (SKA) [187] and the Next-Generation Very Large Array (ngVLA) [188] will have unprecedented sensitivity, excellent angular resolution, and faster survey speed, which will make them ideal for survey studies and transient detections. These new radio facilities are capable of detecting the possible prompt radio burst [189] signals produced by ultra-relativistic jets with timescales of weeks, and by the sub-relativistic merger ejecta with timescales of a few years [33].

Turning to particle detectors, the Cherenkov Telescope Array (CTA) [190] will explore the GeV–TeV sky with a deeper sensitivity than previous instruments. The large field of view, the flexibility to map very large and arbitrary sky patches, and the rapid response time (within about 30 s) make CTA the ideal instrument to detect possible very high energy gamma-ray counterpart of a GW signal. Joint GW-neutrino observations with IceCube and KM3NeT may reveal coincident emissions of high-energy neutrinos from binary neutron star

mergers or other energetic astrophysical phenomena [191].

*Probing SMBBH counterparts* Unlike stellar-mass BHs, SMBH coalescences resulting from the collision and merger of galaxies are expected to take place in environments with significant amounts of gas [192]. This leads to the exciting possibility of electromagnetic signals associated with LISA detections, although the nature of such signals is unclear. Several counterparts, including precursors, prompt transients and afterglows have been proposed in the literature [193], but pinning down the distinctive nature of the emission of an SMBBH coalescences will require detailed general-relativistic magnetohydrodynamic simulations that include radiative transfer, and is currently an active area of theoretical and numerical research [194, 195]. Detecting and identifying EM counterparts of SMBBH coalescences will be challenging. The bulk of LISA events are expected to involve fairly light ($< 10^6$ $M_\odot$), high redshift ($z > 3$) systems, which will make it challenging to achieve a deep coverage on a typical deg$^2$ sky localization with LISA [55]. Nonetheless, the scientific payoffs would be highly valuable, enabling study of the host environment, shedding light on the formation and evolution of SMBHs and their galaxies, allowing for the first time detailed studies of accretion physics on SMBHs of known masses and spins (extracted from the GW signal).

The large population of WD-WD binaries detected by LISA will provide a rich arena for multi-messenger studies [196]. Taking advantage of the complementary nature of EM and GW observations, it will be possible to reveal information about orbital geometries, object sizes, and mass transfer. Unlike many other GW sources, the WD binaries detected by LISA evolve slowly on human time scales, making them persistent multi-messenger sources. In fact, several dozen systems which LISA will observe with high SNR have already been observed electromagnetically [197]. The population of these known "verification binaries" is growing through e.g., the work of the Zwicky Transient Facility [198] and is expected to increase significantly with surveys like GAIA [199] and the Vera C. Rubin Observatory Legacy Survey of Space and Time (LSST) [200] before being greatly expanded by LISA itself.

At nanohertz frequencies PTAs will enable individual detection of several SMBBHs [75, 77] of $M > 10^9$ $M_\odot$ at $z < 1$ in their adiabatic inspiral phase. These are the most massive binaries in the low-redshift Universe, which can only be hosted in extremely massive galaxies. Two possibilities are foreseen for finding individual sources [83]. It will be possible to rank the most likely hosts within the PTA localization area [76] and use time-domain surveys

(such as the Vera Rubin Observatory) as well as available spectroscopic observations to look for periodic, active galactic nuclei (AGN) matching the period of the detected GW, and search for other spectral signatures indicative of a possible binary [201, 202]. The secure identification of counterparts will be critical to understand the distinctive signatures of SMBBHs, distinguishing them from regular AGNs. Those signatures can be then searched for in large AGN data sets to identify the expected much larger population of SMBBHs with periods larger than several years (i.e. emitting GWs below the frequency range probed by PTAs [203]). EM counterpart identification for SMBH coalescences will also enable the study of the host environments of SMBHs, shedding light on the formation and evolution of black holes and their galaxies.

With future radio telescopes like the SKA and the ngVLA, improved timing precision will enable much more precise distance measurements of pulsars used in a PTA [204]. With distances known to within a GW wavelength, the so-called "pulsar term" can be used to determine the position of a single GW to arcsec precision, hence allowing multi-messenger follow-up observations [205].

## FUTURE GRAVITATIONAL-WAVE DETECTORS: CHALLENGES AND APPROACHES

The ambitious GW science opportunities summarized in the previous section will be enabled in coming decade by upgrades to the existing ground-based and PTA detectors and next decade by completely new detectors capable of achieving significant sensitivity increases or, in the case of LISA a completely new observational bands. In the following sections, we survey the needed advances in each detector waveband and discuss the prospects for addressing them.

### Next Generation Ground-based Detectors

The present generation of observatories have arm lengths of 3 km (Advanced Virgo, KAGRA) and 4 km (Advanced LIGO), respectively. Given the fixed arm length $L$, any increase in strain sensitivity for these observatories will be accomplished through reducing displacement noise that limits the measurement precision of $\delta L$. Both Advanced LIGO and

Advanced Virgo are implementing mid-scale upgrade programs, designated A+ and AdV+, that aim to improve the sensitivities of existing observatories by more than 2 times their current levels [206, 207]. The primary planned upgrades include improved mirrors with lower thermal noise optical coatings, better squeezed light performance including frequency dependent optical squeezing [208], and improved GW readout method based on balanced homodyne detection [209, 210]. LIGO-India, slated for operation late in this decade, is planned to come online in the A+ configuration.

Future ground-based detectors are targeting as much as a ten-fold increase in sensitivity over the existing network. The key change will be an increase in the baseline arm length $L$. Two 3rd generation detector concepts – ET in Europe and CE in the US – are currently being pursued in parallel. ET is currently envisioned as an underground infrastructure in Europe housing three interferometers in a triangular configuration each with 10 km arm lengths [91]. CE retains the 'L' interferometer configuration used in the current interferometers but increases the arm lengths to up to 40 km [92]. CE is planned for two-stage implementation: CE1 will primarily use tested Advanced LIGO technology (albeit with heavier mirrors and higher laser power, while CE2 may use newer technologies described in more detail below. Figure 10 displays an artist's conception of ET (left) and compares the Einstein ET and CE configurations and lengths (right). Additionally, external forces on the mirrors will be reduced, via better seismic filtering, reduced thermal noise, and choice of site. Refinements to the sensing system will allow more precise measurements of the positions of the test mirrors, i.e., improving the ability to measure $\delta L$ to further improve their sensitivities.

As compellingly demonstrated by the detection of the binary neutron star merger GW170817 [5], multi-messenger astronomy is one of the driving scientific motivations for building 3rd generation detectors. The angular response (or antenna pattern) of a single interferometer to a GW is essentially omni-directional [19]. To sufficiently resolve the sky location of a GW source, a network of widely separated observatories is needed. As a standalone detector, ET has some capability to identify the sky positions of transient GW sources by virtue of its ability to resolve polarization, while a single CE has very little capability to determine position. To localize sources with $\leq 10$ square degree resolution, at least three interferometers operated as a single global-scale detector are needed.

Designing third generation interferometers, housed in suitable observatories, and capable of meeting the long-term ambitious science goals presented in the previous section, requires

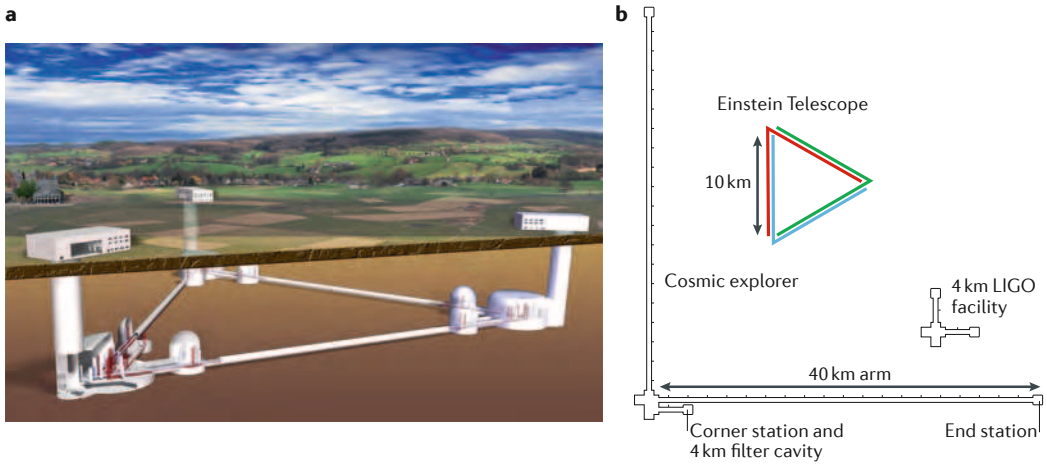


FIG. 10. (Right) Concept for the Einstein Telescope. A triangular underground installation with 10km long arms is planned. The influence of Newtownian noise is reduced with the underground location, and the multiple detectors in the triangular arrangement give a wide sensing bandwidth and polarization resolution. (Left) A comparison of the Einstein Telescope (top) and Cosmic Explorer (bottom) detector configurations. For comparison, the current Advanced LIGO detector is shown for scale.

not only specifying a number of key detector design parameters, but also understanding the interdependencies and design trade-offs to be made:

*Interferometer Arm Length* Increasing the baseline $L$ by lengthening the interferometer arms is perhaps as the strain equation $h = \delta L/L$ implies the easiest path to improved sensitivity. However, increasing the arm length places demands on other detector design aspects. For example, larger beam sizes (due to diffraction of the laser beam) require larger diameter mirrors, placing more stringent requirements on the mirror substrate material and the reflective coating in terms of homogeneity, uniformity and surface figure error. Moreover, when the arm length $L$ approaches the half GW signal wavelength $\lambda = c/f_{GW}$ (where $c$ is the speed of light and $f_{GW}$ is the GW frequency), the sensitivity is reduced. For targeting the detection of the post-merger ringdown of a binary neutron star collision, the sensitivity of the detector at 4kHz is important; a 40km-long arm length reduces the sensitivity for these signals, and a shorter arm length would be better for this particular science goal. In addition, costs for the vacuum system and facility (on the earth's surface or underground) housing the detector scale approximately linearly with length and must be taken into consideration.

Models which combine astrophysical goals and measurement limitations have been developed to determine optimal arm lengths [92].

*Mirror Substrate Material And Temperature* Lowering the mirror temperature can reduce thermal noise both through direct scaling with $\sqrt{kT}$ (here $k$ is the Boltzman constant and $T$ the temperature of the mirror) and through the temperature dependence of the mechanical loss, especially in crystalline materials. While room temperature fused silica is used in most current GW detectors, its performance degrades when cooled. Potential future detector optical substrate materials include crystalline silicon and sapphire, with mirror masses of up to 320 kg currently envisioned to suppress QRPN. Growing single crystal substrates possessing high homogeneity and low optical absorption and low internal stress birefringence will require significant research and development. Ultralow temperatures $\leq 5$ K offer the highest possible reduction in thermal noise; however, the engineering challenges are formidable. As one example, a heat link will be required to extract heat (deposited by the laser interferometer sensing system) from the mirror without introducing excessive displacement noise, thermal noise, or otherwise compromising design requirements. Silicon may have an advantage in that its coefficient of thermal expansion exhibits a zero crossing at 123 K [211], thus reducing thermo-elastic noise [212] and, equally important from an operational standpoint, minimizing thermal lensing induced by heating from light absorption. In addition, it is feasible to extract heat via radiative cooling at 123 K (as the environment can be significantly colder than the substrate), possibly alleviating the need for physically contacted heat links.

*Mirror Coatings* Future interferometers will also require reduced coating thermal noise [10] to achieve their ultimate sensitivity, with the aim of a ten times reduction over the current state of the art. Recent research on ion beam sputtered amorphous coatings has produced factors of a few reduction at 1.06 $\mu$m wavelengths used in today's detectors [213], with evidence that better performance may be achieved out to 2 $\mu$m. Small aperture crystalline coatings have also shown promise [214], but suffer from increased optical loss and challenges in scaling up to large apertures. This appears to be the noise source least susceptible to a straightforward engineering solution. Furthermore, scaling the fabrication process up to coating large optics will require significant engineering development effort.

*Laser Wavelength* Both ET and CE are exploring silicon as a substrate material. However, silicon is opaque at 1.06 $\mu$m (the wavelength used in current detectors), necessitating

the use of wavelengths between 1.5 $\mu$m and 2.1 $\mu$m to be able to transmit light through Fabry-Perot input cavity mirrors, beamsplitters, and auxiliary optics. Longer wavelengths have advantages and disadvantages. They are less susceptible to optical scatter and loss, important for harnessing and preserving the full impact of squeezed quantum states. There may also be evidence of lower coating mechanical loss at longer wavelengths. Conversely, longer wavelengths place tighter requirements on interferometry (the ability to 'split a fringe'). In addition, the diffraction limited beam size increases linearly with wavelengths, requiring larger aperture mirrors. Developing suitably large diameter ($\approx$ 80 cm) and massive silicon substrates with low levels of absorption is a key technology goal for future generation instruments. Finally, frequency-dependent squeezing [215] will be employed to further minimize shot and QRPN. The requisite non-linear optical devices (such as phase modulators) exist at 1.06 $\mu$m, but are in need of significant development at longer wavelengths.

*Laser Power* Shot noise is the dominant limit to interferometer sensitivities at high frequencies in a simple interferometer. The choice of mirror substrate material dictates the choice of laser wavelength, which leads to constraints of laser technologies. Lasers operating at one micron can be scaled to 500W with the required frequency/intensity stability and mode quality [216], however development work is needed to achieve the required power and stability for lasers operating in the 1.5 $\mu$m - 2.1 $\mu$m range.

*Low Frequency Performance* The low frequency observing cutoff is a critical parameter for 3G detectors. Increasing sensitivity to lower frequencies below 10–20 Hz (where the current generation of detectors operate) will enable detections of intermediate mass black holes mergers (in the range of $10^2$ - $10^4$ $M_\odot$) and shed light on how heavier black holes form. Mirror suspensions systems currently have fundamental resonances in the 1 Hz range; future detectors' suspensions must push to lower resonant frequencies for greater isolation in the 1 - 10 Hz range. Suspension stages may need to be made from silicon or sapphire that can be cooled to reduce thermal noise. Minimizing Newtonian noise necessitates finding a site with low environmental noise. An underground location (as is planned for ET) should reduce the Newtonian noise, although requiring care in preserving the quiet environment through observatory design. In addition, Newtonian noise subtraction approaches [217] need to be designed and tested to reach the planned factor of 10 reduction to meet ET and CE performance goals.

*Observatory Network Configuration* Multi-messenger astronomy requires accurate and relatively precise localization of GW events. The current network currently has four km-scale observatories in operation – LIGO Hanford, LIGO Livingston, Virgo, and KAGRA. The addition of LIGO-India later this decade will further improve the sky localization capability [19]. Detailed studies of networks [218] show that a third detector to complement ET or CE in the southern hemisphere – needed for detecting events with error boxes less than 10 square degrees – would form a powerful array, and studies are ongoing in e.g., Australia for possible implementation.

*Interferometer Vacuum Systems* Observatory vacuum systems are a critical infrastructure component for 3G observatories. The laser light used to probe the arm lengths must travel in an ultrahigh vacuum to avoid path-length fluctuations due to the polarizability of residual gas, and the beam tube must not introduce scattered light. As it is currently envisioned, CE will require two 40 km beam tubes, of 1.2 m diameter, at pressures less than $10^{-9}$ torr with stringent requirements on partial pressures of molecular hydrogen, water, and select hydrocarbons. The vacuum system comprises much of the cost of a 3G observatory. Thus, 'value engineering' vacuum systems is a high priority. Efforts are already underway exploring the use of low carbon steel as well as the use of nested vacuum systems [219].

*Civil Engineering:* Whether the new observatories are nominally on the surface of the earth (e.g., CE) or underground (e.g., ET), there will be significant costs associated with the civil engineering. Site location, acquisition, and preparation can present significant practical challenges, and can impact the configuration of a world-wide array.

Addressing these primary challenges (and a myriad of other challenges not discussed here) will require a sustained and globally coordinated R&D program to be undertaken before ET and CE conceptual designs can be finalized. To have operating 3G detectors in the 2030s, facility construction should commence in this decade, requiring R&D and prototyping efforts currently underway to be ramped up significantly. Several efforts are of sufficiently large scale that industrial partnerships will be essential to succeed. Examples include the development of mirror optical coatings and mirror substrates with the requisite optical and mechanical properties. Also essential in the near term is the development of a prototype interferometer testbed for interferometry and laser development at laboratory scale.

On a longer term, upgrading one or more of the existing LIGO facilities to a full km-scale interferometer using 3G technologies is particularly appealing path to a full scale 3G

interferometer network in that it will both test 3G technologies almost 'at scale' and deliver a detector with considerably more sensitivity than the current second generation detectors. The LIGO Voyager detector design [93] is being explored as a possible upgrade to the existing LIGO Observatories late in this decade. Voyager can potentially achieve a two-fold sensitivity increase when compared against Advanced LIGO Plus. In addition, the Neutron star Extreme Matter Observatory (NEMO [220]) has been proposed in Australia as a 4km observatory targeting neutron star GW astrophysics, aiming to have sensitivity comparable to ET and CE at frequencies above 2 kHz.

**Future Space-based Detectors**

Space-based detectors measure differential strain using an approach that is similar to that of their terrestrial counterparts. The primary difference between space-based designs such as LISA [54] (Figure 11) and terrestrial interferometers is the size of the baselines: $L$ is currently 3 or 4 km for existing ground-based designs with plans for 10 or 40 km for future designs, versus $L \sim 2.5 \times 10^6$ km for the LISA design. The longer baselines has two effects. First, the required displacement sensitivity of the interferometric metrology system to achieve an equivalent GW strain sensitivity is roughly a factor of a million less for space-based interferometers than ground-based interferometers. Secondly, the optimal response to GWs is shifted to the milliHertz frequency band, roughly the inverse of the light travel time across the $\sim 10^9$ m baselines. These differences change the nature of the noise sources which limit the instrument's response. Many of the fundamental limitations on measurement such as seismic noise, and thermal noise in optics and coatings that must be cleverly addressed in ground-based interferometers, are not an issue for space-based interferometers due to the larger size of the displacements. On the other hand, the longer wave periods (hours to seconds) and increased duration of the signals (hours to years) demand that the designers of space-based interferometers must be more concerned with the very low frequency gravitational and electromagnetic stochastic forces due to thermal drifts. And of course the space-based instruments must operate in, and protect their test masses from, the harsh environment of space and without direct human intervention.

Aside from these differences between ground- and space-based GW interferometers, the fundamental limitations on sensitivity are the same; stray forces on the test masses, and a

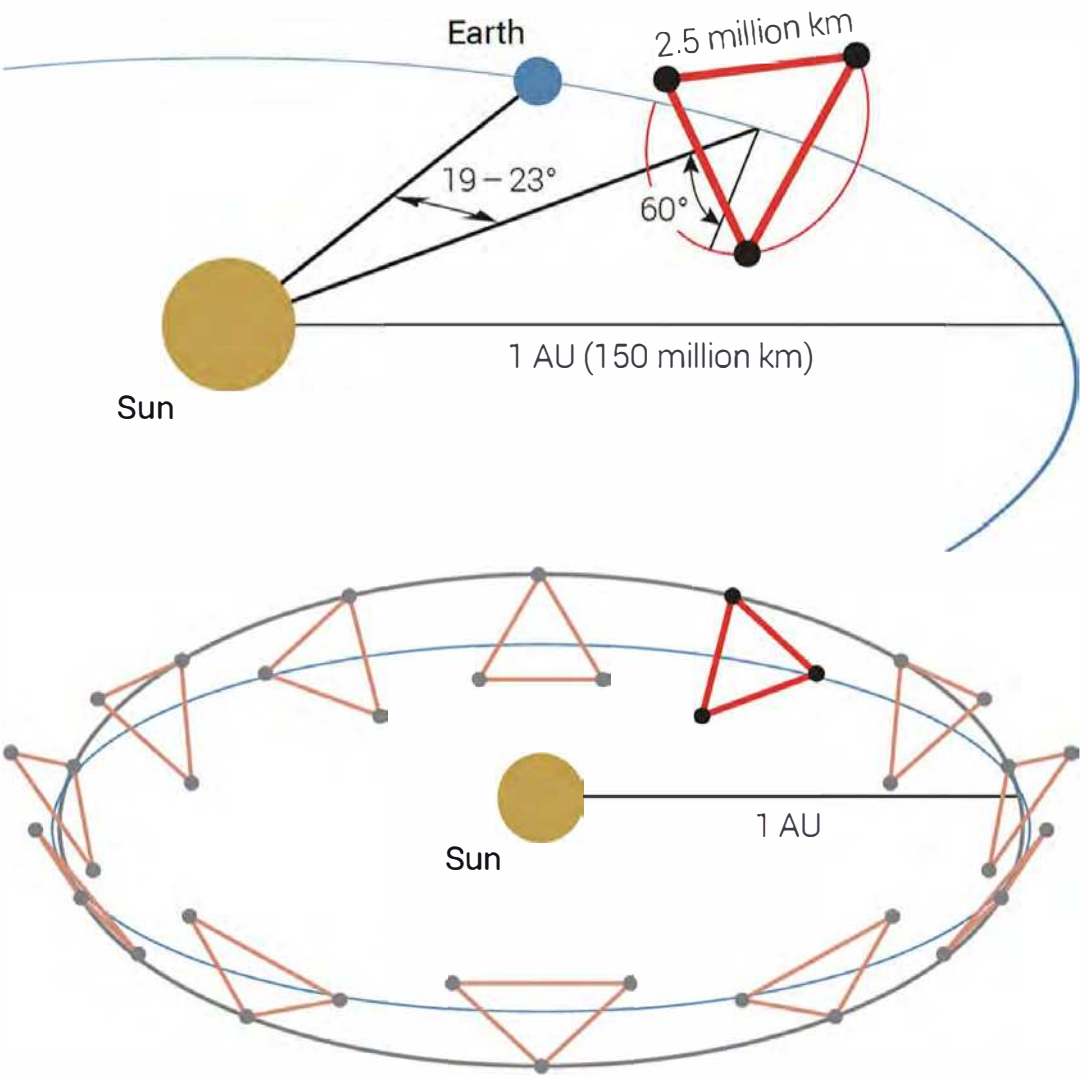


FIG. 11. The LISA Mission. Top: Three spacecraft, in a triangular stable orbit, are separated by $2.5 \times 10^6$ km. Laser beams measure between each spacecraft in both directions; from these 6 legs distortions due to passing GWs in both polarizations can be resolved. Bottom: A 1 AU orbit is chosen, and the constellation scans the sky once per year. *Credit: LISA Consortium*

limited precision in the measurement of the separation of the test masses.

The first limit is how well the test masses, which act as a fiducial inertial test particle, approximate an inertial frame. This can be characterized by the spectrum of residual acceleration from non-gravitational forces on the test mass. For first-generation space-based interferometers, the required level of accelerations is on the order of femto-g's ($1\,\mathrm{g} = 9.81/\mathrm{m/s^2}$). The specific requirement for LISA is for the non-gravitational forces on each test mass to

be less than $3 \times 10^{-15}\,\mathrm{m/s^2/Hz^{1/2}}$ in the millihertz band, with relaxations at both higher and lower frequencies [54]. When expressed as an acceleration, this is similar to the stability of the test masses in the second-generation ground-based interferometers which made the historic first detections of GWs.

A practical consequence of working in space is that the strength of the local gravitational field, which is $\sim 1\,\mathrm{g}$ for ground-based interferometers, is significantly lower – typically limited by the mass distribution of the spacecraft itself (and perhaps nearby celestial bodies depending on the orbit). This allows a conceptually simple technique to be used to realize the low-disturbance test mass: simply let go of it and let it drift. Forces from sunlight and residual particles in the space environment can be avoided by allowing the test mass to drift within a shielded housing inside the spacecraft. To keep the spacecraft from running into the test mass, and to limit disturbances from electrostatic and gravitational couplings between the spacecraft and test mass, a control system known as drag-free control is used to precisely steer the spacecraft to follow the test mass [221]. Drag-free control was incorporated into early design concepts for space-based interferometers, and was first demonstrated by the LPF spacecraft in 2016 [222, 223]. At the core of LPF were two Gravitational Reference Sensors (GRS), each consisting of a test mass, an electrostatic sensing and control assembly, and a surrounding vacuum enclosure. The test masses were cubes of a gold-platinum alloy, approximately 4 cm on a side and with a mass of $\sim 2\,\mathrm{kg}$ (Figure 12). These were separated from their hollow cubic housing by gaps of a few millimeters. Electrodes on the inner faces of the housing allowed the position and orientation of the test mass to be both sensed in all six kinematic degrees of freedom. These same electrodes could be used to apply forces and torques to the test mass electrostatically. The two GRS assemblies were placed approximately 38 cm apart with a optical bench placed between them. This optical bench was used to perform a series of interferometric measurements to determine the relative position of the two test masses as well as the position of one test mass relative to the spacecraft. During LPF operations, the spacecraft operated in drag-free mode around one of the two test masses, with the second test mass electrostatically suspended as a witness. While the design requirements for LPF were deliberately relaxed from those of LISA, LPF performed far better than the pathfinder requirements (Figure 12), and was able to demonstrate a performance that was significantly better than the LISA requirements [222, 223].

Relative to ground-based interferometers, the scale of the GW-induced displacements in

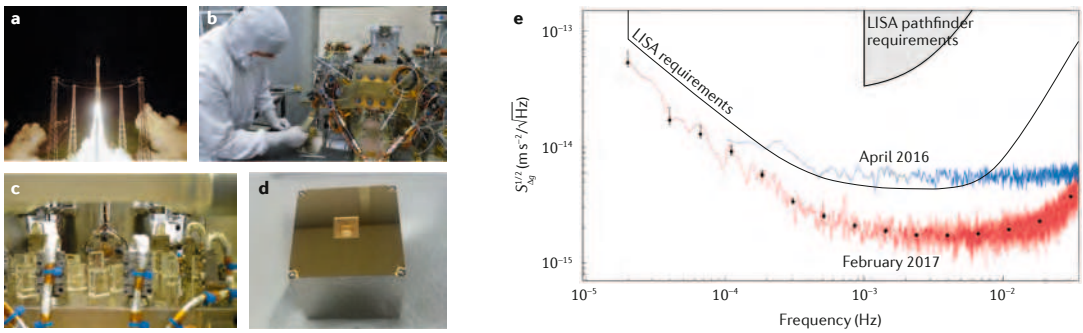


FIG. 12. LISA Pathfinder technology and performance. The left figures display (clockwise from upper left) the launch of the LISA Pathfinder Mission in December 2015, the LP core assembly, one of the two test masses in the core assembly, and a close up of the LP optical bench used to read out the relative test mass displacement noise. The right graph shows the measured acceleration noise of the LISA Pathfinder Mission. The vertical scale is the relative acceleration noise amplitude spectral density between the two GRS test masses. The LPF demonstrator performed far better than its requirements, and exceeded the LISA flight requirements in the relevant low-frequency regime.

space-based interferometers is significantly larger ($\sim 10^{-12}$ m for space-based vs. $\sim 10^{-18}$ m for ground-based). As a result, the interferometric techniques for space are comparatively simple – there is no need for resonant cavities and complex interferometer topologies such as power and signal recycling cavities as shown in figure 4. On the other hand, the measurement must be made over long distances and between separate platforms with large relative motion. For LISA, the relative velocity between each pair of spacecraft is several m/s over the separation distance of $\sim 2.5 \times 10^6$. The first challenge is simply getting enough light from one spacecraft to another. Using a 30 cm telescope to both transmit and receive the beam on each spacecraft, diffraction over these baselines results in a reduction in power of roughly $10^{10}$ at the collection point. To reach a shot-noise limited displacement noise in the picometer range (1 pm $= 10^{-12}$ m) requires that roughly 1 W of 1 $\mu$m laser light leave the telescope. This is a moderately high level for space-qualified continuous-wave lasers and likely requires the use of a multi-stage laser system. Because of these large diffraction losses, there is no hope of reflecting the light back to the originating spacecraft as would be done in a classical Michelson interferometer. Instead, a triangular constellation of three identical satellites is used. Each spacecraft simultaneously transmits its own laser signal while receiving signals

from each of other two in the constellation. The incoming and outgoing beams are brought to interference on a optical bench, resulting in a fringe pattern that encodes information about each laser's intrinsic frequency noise, the orbital motion of the spacecraft, and small fluctuations from passing GWs. These fringe patterns are tracked and recorded on each of the three satellites and transmitted to ground. The set of measurements is then combined using a technique called Time Delay Interferometry (TDI) in which linear combinations of each signal are formed that suppress the intrinsic phase noise of the lasers while retaining the GW information [224, 225].

The basic principles of the LISA displacement measurement have been validated through a combination of numerical experiments [226] and demonstrations using laboratory analogs [227, 228]. More recently, an opportunity to validate several key components of the LISA metrology system in flight has been realized with the Laser Ranging Instrument (LRI) on board the GRACE-Follow On (GRACE-FO) which measures the distance between two satellites via optical interferometry. Several of the LRI parameters, including the delivered light powers, Doppler rates, and laser phase noise, are similar to those for LISA. The first LRI results demonstrate nanometer-level ranging over the 210 km link, meeting the design goals of LRI and within a few orders of magnitude of the LISA requirements despite LRI operating with a single link and therefore being limited by laser frequency noise [229].

The current planned launch date for LISA is 2034 to match ESA's schedule for its 'L' (Large) missions. ESA and its European and US partners are currently engaged in a concerted effort to complete developments of technologies that were not demonstrated on LPF or GRACE-FO or which require minor modifications. These developments will be completed by the time the mission enters its implementation phase, planned for the mid-2020s. While on-time launch of LISA appears feasible, LISA may not be the sole member of the first generation of space-based GW observatories. Several Chinese-led efforts are currently in development, including the *TianQin* [230] concept for a geocentric constellation and the *Taiji* [231] concept for a heliocentric constellation, both of which employ an architecture similar to LISA but with somewhat different instrumental parameters.

To reach sensitivities beyond this first generation of observatories will require additional investments in basic research. Concepts for second-generation space-based GW observatories include ones targeting frequency bands above [232] and below that of LISA. Deci-hertz Interferometer Gravitational Wave Observatory (DECIGO) [233, 234] is the future Japanese space

mission with a frequency band of 0.1 Hz to 10 Hz, mainly aiming at the detection of primordial GWs. DECIGO consists of three spacecraft, which form three Fabry-Perot Michelson interferometers with an arm length of 1,000 km. Concepts beyond that of LISA [235] to look at even more massive systems have also been discussed, as well as detectors similar to LISA with increased sensitivity [236]. An alternative possibility would be the deployment of networks of space-based observatories, which could greatly improve angular resolution and enable further multimessenger science [237]. The specific technology required would depend on the science target and mission architecture. Examples include more powerful and yet stable lasers, large but still dimensionally stable telescopes, inertial sensors with even better performance than those flown on LPF, or perhaps more compact and affordable elements that would allow for large networks of space-based interferometers to be deployed.

**Future Pulsar Timing Arrays**

In the near term, improvements to the PTA network will focus on improved receivers with much wider radio bandwidths being developed and deployed on several telescopes [238]. These will increase sensitivity dramatically by allowing better removal of interstellar propagation effects and integrating more of the emitted radio signals. Wider bandwidth receivers will also allow for greater observing efficiency, obviating the need for observations at multiple frequencies. These new facilities and instruments will greatly enhance the sensitivity of the individual and global PTAs, but will also increase the already difficult task of merging the heterogeneous data from all of the individual telescopes in the array; due to this difficulty the current best IPTA limits on the stochastic GW background are less constraining than the best individual PTA limit [81].

Significant human and computational resources will be needed needed to make the IPTA project a success. Recently, great progress has been made in developing new GW detection algorithms that properly account for a number of sources of noise in PTA data. As an example, planetary ephemermides have been found to be too inaccurate for PTA experiments, but a new software package can properly model these ephemeris errors while performing the GW searches [81, 239].

Other issues that must be carefully considered include long-term pulse profile evolution, our ability to accurately model changes in the electron column density along the line of sight,

and pulse jitter (pulse-pulse deviations from the average). Pulse jitter is pulsar-dependent, and defines a minimum dwell time regardless of telescope sensitivity to achieve a given timing precision. For the celebrated bright millisecond pulsar PSR J0437–4715, observations of less than an hour can never achieve residuals below 40 ns. Others, such as PSR J1909–3744 have much lower levels of jitter, nearer 10 ns. Timing arrays are starting to factor jitter limits into their observing plans so that large aperture facilities are not "wasted" on targets that do not benefit from increased signal-to-noise ratios.

Looking further into the future (e.g. [240]), the Square Kilometre Array and the proposed ngVLA will further enhance detection and science prospects, and China has other large-aperture radio telescopes planned like the 110 m Xingjiang QTT. Existing timing limits are near where many models predicted the stochastic background might be, and there is a good chance that an individual source may be separable from the background within the next decade. The major threat to pulsar timing array science is the increasingly-crowded radio spectrum from satellites, aircraft, and ground-based transmitters that increasingly use the once-sparsely populated 300 MHz-3 GHz band for terrestrial navigation and communications.

## CONCLUSIONS

With just a few years of instruments capable of recording the waveforms of signals, the ground-based detectors have made seminal contributions to the fields of GR, fundamental physics, and astrophysics. The multi-messenger characterization of the first observable binary neutron star coalescence dramatically enhanced our understanding of extreme states of nuclear matter and the astrophysics of kilonovae.

The scientific potential for the field of GW science in the next few decades is considerable, afforded by the prospects of upgrades to existing observatories in this decade and the construction or launch of new observatories in the 2030s. There are clear paths to improvements in both the sensitivity of the instruments and the range of frequencies: for ground-based detectors, sensitive to astrophysics of up to $\sim$1000 stellar mass compact objects, we will see the network of detectors of 3- and 4-km scale both improve and grow in the coming decade, and the future planned ET and CE observatories offer the possibility of a quieter environment, implementation of detectors of greater complexity, and longer arms; all stellar-mass coalescing BBH systems in the Universe will be within reach. The

LISA space-based detector will deliver sensitivity to signals from super-massive black holes, with exquisite resolution of signal waveforms and completing the survey of the Universe for binaries up to some $10^6$ solar masses. The pulsar timing arrays will continue to evolve with new antenna networks, more sensitive and wider-band receivers, and discovery of additional pulsar 'clocks', giving unique information on the dynamics of the very largest galaxies in the Universe. Together with electromagnetic and particle detectors these instruments will provide quantitative *and* qualitative new insights into physics, astrophysics, cosmology, and astronomy. Gravitational-wave detectors have indeed opened a new window onto the Universe.

[1] Einstein, A. Approximative integration of the field equations of gravitation. *Sitzungsber. K. Preuss. Akad. Wiss.* **1**, 688–696 (1916).

[2] Aasi, J. *et al.* Advanced ligo. *Classical and quantum gravity* **32**, 074001 (2015).

[3] Abbott, B. P. *et al.* Observation of gravitational waves from a binary black hole merger. *Physical review letters* **116**, 061102 (2016).

[4] Acernese, F. *et al.* Advanced virgo: a second-generation interferometric gravitational wave detector. *Classical and Quantum Gravity* **32**, 024001 (2014).

[5] Abbott, B. P. *et al.* Gw170817: Observation of gravitational waves from a binary neutron star inspiral. *Physical Review Letters* **119**, 161101 (2017).

[6] Abbott, B. P. *et al.* Multi-messenger Observations of a Binary Neutron Star Merger. *The Astrophysical Journal Letters* **848**, L12 (2017). 1710.05833.

[7] URL `https://gwic.ligo.org`.

[8] Marx, J. *et al.* The future of gravitational wave astronomy (2010). URL `https://gwic.ligo.org/roadmap/Roadmap_110726_WEB.pdf`.

[9] Matichard, F. *et al.* Seismic isolation of advanced LIGO: Review of strategy, instrumentation and performance. *Classical and Quantum Gravity* **32**, 185003 (2015).

[10] Harry, G., Bodiya, T. P. & DeSalvo, R. *Optical coatings and thermal noise in precision measurement* (Cambridge University Press, 2012).

[11] Beker, M. G. *et al.* Improving the sensitivity of future gw observatories in the 1–10 hz band: Newtonian and seismic noise. *General Relativity and Gravitation* **43**, 623–656 (2011).

[12] Hughes, S. A. & Thorne, K. S. Seismic gravity-gradient noise in interferometric gravitational-wave detectors. *Phys. Rev. D* **58**, 122002 (1998). gr-qc/9806018.

[13] Tse, M. *et al.* Quantum-enhanced advanced LIGO detectors in the era of gravitational-wave astronomy. *Physical Review Letters* **123** (2019).

[14] Harry, G. M. *et al.* Thermal noise from optical coatings in gravitational wave detectors. *Applied Optics* **45**, 1569 (2006).

[15] Abbott, R. *et al.* Gwtc-2: Compact binary coalescences observed by ligo and virgo during the first half of the third observing run. *arXiv preprint arXiv:2010.14527* (2020).

[16] Aso, Y. *et al.* Interferometer design of the kagra gravitational wave detector. *Physical Review*

*D* **88**, 043007 (2013).

[17] Akutsu, T. *et al.* Kagra: 2.5 generation interferometric gravitational wave detector. *Nature Astronomy* **3**, 35–40 (2019). URL `https://doi.org/10.1038/s41550-018-0658-y`.

[18] Unnikrishnan, C. Indigo and ligo-india: Scope and plans for gravitational wave research and precision metrology in india. *International Journal of Modern Physics D* **22**, 1341010 (2013).

[19] Fairhurst, S. Localization of transient gravitational wave sources: beyond triangulation. *Classical and Quantum Gravity* **35**, 105002 (2018).

[20] Raffai, P. *et al.* Optimal networks of future gravitational-wave telescopes. *Classical and Quantum Gravity* **30**, 155004 (2013).

[21] Abbott, B. *et al.* Gw151226: Observation of gravitational waves from a 22-solar-mass binary black hole coalescence. *Physical Review Letters* **116**, 241103 (2016).

[22] Abbott, B. *et al.* Binary black hole mergers in the first advanced ligo observing run. *Physical Review X* **6**, 041015 (2016).

[23] Abbott, B. P. *et al.* Gw170814: a three-detector observation of gravitational waves from a binary black hole coalescence. *Physical review letters* **119**, 141101 (2017).

[24] Abbott, B. *et al.* Gw170608: Observation of a 19 solar-mass binary black hole coalescence. *The Astrophysical Journal Letters* **851**, L35 (2017).

[25] Abbott, B. P. *et al.* Astrophysical implications of the binary black-hole merger gw150914. *The Astrophysical Journal* **818**, L22 (2016).

[26] Abbott, B. P. *et al.* Binary black hole population properties inferred from the first and second observing runs of advanced LIGO and advanced virgo. *The Astrophysical Journal* **882**, L24 (2019).

[27] Abbott, B. *et al.* GWTC-1: A gravitational-wave transient catalog of compact binary mergers observed by LIGO and virgo during the first and second observing runs. *Physical Review X* **9** (2019).

[28] Abbott, R. *et al.* Gw190521: A binary black hole merger with a total mass of 150 $m_{\odot}$. *Physical Review Letters* **125**, 101102 (2020).

[29] Abbott, R. *et al.* Properties and astrophysical implications of the 150 $m_{\odot}$ binary black hole merger gw190521. *The Astrophysical Journal Letters* **900**, L13 (2020).

[30] Abbott, B. *et al.* Gravitational waves and gamma-rays from a binary neutron star merger: Gw170817 and grb 170817a. *The Astrophysical Journal Letters* **848**, L13 (2017).

[31] Goldstein, A. *et al.* An ordinary short gamma-ray burst with extraordinary implications: Fermi-gbm detection of grb 170817a. *The Astrophysical Journal Letters* **848**, L14 (2017).

[32] Troja, E. *et al.* The x-ray counterpart to the gravitational-wave event GW170817. *Nature* **551**, 71–74 (2017).

[33] Hotokezaka, K. *et al.* Radio Counterparts of Compact Binary Mergers Detectable in Gravitational Waves: A Simulation for an Optimized Survey. *The Astrophysical Journal* **831**, 190 (2016). 1605.09395.

[34] Coulter, D. *et al.* Swope supernova survey 2017a (sss17a), the optical counterpart to a gravitational wave source. *Science* **358**, 1556–1558 (2017).

[35] Soares-Santos, M. *et al.* The electromagnetic counterpart of the binary neutron star merger ligo/virgo gw170817. i. discovery of the optical counterpart using the dark energy camera. *The Astrophysical Journal Letters* **848**, L16 (2017).

[36] Valenti, S. *et al.* The discovery of the electromagnetic counterpart of gw170817: kilonova at 2017gfo/dlt17ck. *The Astrophysical Journal Letters* **848**, L24 (2017).

[37] McCully, C. *et al.* Optical emission from a kilonova following a gravitational-wave-detected neutron-star merger. *Nature* **551**, 64 (2017).

[38] Tanvir, N. *et al.* The emergence of a lanthanide-rich kilonova following the merger of two neutron stars. *The Astrophysical Journal Letters* **848**, L27 (2017).

[39] Lipunov, V. *et al.* Master optical detection of the first ligo/virgo neutron star binary merger gw170817. *The Astrophysical Journal Letters* **850**, L1 (2017).

[40] Margutti, R. *et al.* The binary neutron star event LIGO/virgo GW170817 160 days after merger: Synchrotron emission across the electromagnetic spectrum. *The Astrophysical Journal* **856**, L18 (2018).

[41] Lyman, J. D. *et al.* The optical afterglow of the short gamma-ray burst associated with GW170817. *Nature Astronomy* **2**, 751–754 (2018).

[42] Mooley, K. P. *et al.* Superluminal motion of a relativistic jet in the neutron-star merger GW170817. *Nature* **561**, 355–359 (2018).

[43] Ghirlanda, G. *et al.* Compact radio emission indicates a structured jet was produced by a binary neutron star merger. *Science* **363**, 968–971 (2019).

[44] Drout, M. *et al.* Light curves of the neutron star merger gw170817/sss17a: Implications for r-process nucleosynthesis. *Science* eaaq0049 (2017).

[45] Chornock, R. *et al.* The electromagnetic counterpart of the binary neutron star merger ligo/virgo gw170817. iv. detection of near-infrared signatures of r-process nucleosynthesis with gemini-south. *The Astrophysical Journal Letters* **848**, L19 (2017).

[46] Kasliwal, M. *et al.* Illuminating gravitational waves: a concordant picture of photons from a neutron star merger. *Science* **358**, 1559–1565 (2017).

[47] Pian, E. *et al.* Spectroscopic identification of r-process nucleosynthesis in a double neutron-star merger. *Nature* **551**, 67–70 (2017).

[48] Smartt, S. J. *et al.* A kilonova as the electromagnetic counterpart to a gravitational-wave source. *Nature* **551**, 75–79 (2017).

[49] Watson, D. *et al.* Identification of strontium in the merger of two neutron stars. *Nature* **574**, 497–500 (2019).

[50] Schutz, B. F. Determining the hubble constant from gravitational wave observations. *Nature* **323**, 310 (1986).

[51] Abbott, B. P. *et al.* A gravitational-wave standard siren measurement of the Hubble constant. *Nature* **551**, 85–88 (2017). 1710.05835.

[52] Abbott, B. *et al.* Tests of general relativity with gw150914. *Physical Review Letters* **116**, 221101 (2016).

[53] Abbott, B. P. *et al.* Gw170817: implications for the stochastic gravitational-wave background from compact binary coalescences. *Physical review letters* **120**, 091101 (2018).

[54] Amaro-Seoane, P. *et al.* Laser Interferometer Space Antenna. *ArXiv e-prints* (2017). 1702.00786.

[55] Klein, A. *et al.* Science with the space-based interferometer elisa: Supermassive black hole binaries. *Physical Review D* **93**, 024003 (2016).

[56] Amaro-Seoane, P. *et al.* Intermediate and extreme mass-ratio inspirals—astrophysics, science applications and detection using lisa. *Classical and Quantum Gravity* **24**, R113 (2007).

[57] Sesana, A. Prospects for multiband gravitational-wave astronomy after gw150914. *Physical Review Letters* **116**, 231102 (2016).

[58] Nissanke, S., Vallisneri, M., Nelemans, G. & Prince, T. A. Gravitational-wave Emission from Compact Galactic Binaries. *The Astrophysical Journal* **758**, 131 (2012). 1201.4613.

[59] Armano, M. *et al.* Beyond the required lisa free-fall performance: New lisa pathfinder results down to 20$\mu$Hz. *Phys. Rev. Lett.* **120**, 061101 (2018). URL `https://link.aps.org/doi/10.`

1103/PhysRevLett.120.061101.

[60] McLaughlin, M. A. The north american nanohertz observatory for gravitational waves. *Classical and Quantum Gravity* **30**, 224008 (2013).

[61] Kramer, M. & Champion, D. J. The european pulsar timing array and the large european array for pulsars. *Classical and Quantum Gravity* **30**, 224009 (2013).

[62] Manchester, R. *et al.* The parkes pulsar timing array project. *Publications of the Astronomical Society of Australia* **30** (2013).

[63] Verbiest, J. *et al.* The international pulsar timing array: first data release. *Monthly Notices of the Royal Astronomical Society* **458**, 1267–1288 (2016).

[64] Sazhin, M. V. Opportunities for detecting ultralong gravitational waves. *Soviet Astronomy* **22**, 36–38 (1978).

[65] Detweiler, S. Pulsar timing measurements and the search for gravitational waves. *ApJ* **234**, 1100–1104 (1979).

[66] Lorimer, D. R. & Kramer, M. *Handbook of Pulsar Astronomy* (2004).

[67] Hellings, R. W. & Downs, G. S. Upper limits on the isotopic gravitational radiation background frompulsar timing analysis. *The Astrophysical Journal Letters* **265**, L39–L42 (1983).

[68] Hobbs, G. The Parkes Pulsar Timing Array. *Classical and Quantum Gravity* **30**, 224007 (2013). 1307.2629.

[69] Kramer, M. & Champion, D. J. The European Pulsar Timing Array and the Large European Array for Pulsars. *Classical and Quantum Gravity* **30**, 224009 (2013).

[70] Ransom, S. *et al.* The NANOGrav Program for Gravitational Waves and Fundamental Physics. In *Bulletin of the American Astronomical Society*, vol. 51, 195 (2019). 1908.05356.

[71] Manchester, R. N. & IPTA. The International Pulsar Timing Array. *Classical and Quantum Gravity* **30**, 224010 (2013). 1309.7392.

[72] Sesana, A., Vecchio, A. & Colacino, C. N. The stochastic gravitational-wave background from massive black hole binary systems: implications for observations with Pulsar Timing Arrays. *Monthly Notices of the Royal Astronomical Society* **390**, 192–209 (2008). 0804.4476.

[73] Rosado, P. A., Sesana, A. & Gair, J. Expected properties of the first gravitational wave signal detected with pulsar timing arrays. *Monthly Notices of the Royal Astronomical Society* **451**, 2417–2433 (2015). 1503.04803.

[74] Taylor, S. R. *et al.* Are We There Yet? Time to Detection of Nanohertz Gravitational Waves

Based on Pulsar-timing Array Limits. *Astrophys. J. Lett.* **819**, L6 (2016). 1511.05564.

[75] Sesana, A., Vecchio, A. & Volonteri, M. Gravitational waves from resolvable massive black hole binary systems and observations with Pulsar Timing Arrays. *Monthly Notices of the Royal Astronomical Society* **394**, 2255–2265 (2009). 0809.3412.

[76] Mingarelli, C. M. F. *et al.* The local nanohertz gravitational-wave landscape from supermassive black hole binaries. *Nature Astronomy* **1**, 886–892 (2017). 1708.03491.

[77] Kelley, L. Z., Blecha, L., Hernquist, L., Sesana, A. & Taylor, S. R. Single sources in the low-frequency gravitational wave sky: properties and time to detection by pulsar timing arrays. *Monthly Notices of the Royal Astronomical Society* **477**, 964–976 (2018). 1711.00075.

[78] Milosavljević, M. & Merritt, D. The final parsec problem. In *AIP Conference Proceedings*, vol. 686, 201–210 (AIP, 2003).

[79] Shannon, R. M. *et al.* Gravitational waves from binary supermassive black holes missing in pulsar observations. *Science* **349**, 1522–1525 (2015).

[80] Lentati, L. *et al.* European Pulsar Timing Array limits on an isotropic stochastic gravitational-wave background. *Monthly Notices of the Royal Astronomical Society* **453**, 2576–2598 (2015). 1504.03692.

[81] Arzoumanian, Z. *et al.* The NANOGrav 11 Year Data Set: Pulsar-timing Constraints on the Stochastic Gravitational-wave Background. *ApJ* **859**, 47 (2018). 1801.02617.

[82] Middleton, H., Chen, S., Del Pozzo, W., Sesana, A. & Vecchio, A. No tension between assembly models of super massive black hole binaries and pulsar observations. *Nature Communications* **9**, 573 (2018). 1707.00623.

[83] Burke-Spolaor, S. *et al.* The astrophysics of nanohertz gravitational waves. *The Astronomy and Astrophysics Review* **27**, 5 (2019). 1811.08826.

[84] Maggiore, M. Gravitational wave experiments and early universe cosmology. *Physics Reports* **331**, 283–367 (2000).

[85] Caprini, C. & Figueroa, D. G. Cosmological backgrounds of gravitational waves. *Classical and Quantum Gravity* **35**, 163001 (2018). 1801.04268.

[86] Kamionkowski, M. & Kosowsky, A. Detectability of inflationary gravitational waves with microwave background polarization. *Phys. Rev. D* **57**, 685–691 (1998). astro-ph/9705219.

[87] Sathyaprakash, B. *et al.* Extreme Gravity and Fundamental Physics (2019). 1903.09221.

[88] Sathyaprakash, B. *et al.* Multimessenger Universe with Gravitational Waves from Binaries

(2019). 1903.09277.

[89] Kalogera, V. *et al.* Deeper, Wider, Sharper: Next-Generation Ground-Based Gravitational-Wave Observations of Binary Black Holes (2019). 1903.09220.

[90] Sathyaprakash, B. *et al.* Cosmology and the Early Universe (2019). 1903.09260.

[91] Punturo, M. *et al.* The einstein telescope: a third-generation gravitational wave observatory. *Classical and Quantum Gravity* **27**, 194002 (2010).

[92] BP, A. *et al.* Exploring the sensitivity of next generation gravitational wave detectors. *Classical and Quantum Gravity* **34**, 18 (2017).

[93] Adhikari, R. X. *et al.* A cryogenic silicon interferometer for gravitational-wave detection (2020). 2001.11173.

[94] Will, C. M. The Confrontation between General Relativity and Experiment. *Living Rev. Rel.* **17**, 4 (2014). 1403.7377.

[95] Gair, J. R., Vallisneri, M., Larson, S. L. & Baker, J. G. Testing General Relativity with Low-Frequency, Space-Based Gravitational-Wave Detectors. *Living Rev. Rel.* **16**, 7 (2013). 1212.5575.

[96] Yunes, N. & Siemens, X. Gravitational-Wave Tests of General Relativity with Ground-Based Detectors and Pulsar Timing-Arrays. *Living Rev. Rel.* **16**, 9 (2013). 1304.3473.

[97] Berti, E. *et al.* Testing General Relativity with Present and Future Astrophysical Observations. *Class. Quant. Grav.* **32**, 243001 (2015). 1501.07274.

[98] Unruh, W. G. & Wald, R. M. Information Loss. *Rept. Prog. Phys.* **80**, 092002 (2017). 1703.02140.

[99] Penrose, R. Gravitational collapse and space-time singularities. *Phys. Rev. Lett.* **14**, 57–59 (1965).

[100] Hawking, S. & Penrose, R. The Singularities of gravitational collapse and cosmology. *Proc. Roy. Soc. Lond. A* **314**, 529–548 (1970).

[101] Riess, A. G. *et al.* Observational evidence from supernovae for an accelerating universe and a cosmological constant. *Astron. J.* **116**, 1009–1038 (1998). astro-ph/9805201.

[102] Perlmutter, S. *et al.* Measurements of $\Omega$ and $\Lambda$ from 42 high redshift supernovae. *Astrophys. J.* **517**, 565–586 (1999). astro-ph/9812133.

[103] Peebles, P. & Ratra, B. The Cosmological Constant and Dark Energy. *Rev. Mod. Phys.* **75**, 559–606 (2003). astro-ph/0207347.

[104] Riess, A. G., Casertano, S., Yuan, W., Macri, L. M. & Scolnic, D. Large Magellanic Cloud Cepheid Standards Provide a 1% Foundation for the Determination of the Hubble Constant and Stronger Evidence for Physics beyond ΛCDM. *Astrophys. J.* **876**, 85 (2019). 1903.07603.

[105] de Swart, J., Bertone, G. & van Dongen, J. How Dark Matter Came to Matter. *Nature Astron.* **1**, 0059 (2017). 1703.00013.

[106] Burgay, M. *et al.* An Increased estimate of the merger rate of double neutron stars from observations of a highly relativistic system. *Nature* **426**, 531–533 (2003). astro-ph/0312071.

[107] Bertotti, B., Iess, L. & Tortora, P. A test of general relativity using radio links with the Cassini spacecraft. *Nature* **425**, 374–376 (2003).

[108] Akiyama, K. *et al.* First M87 Event Horizon Telescope Results. I. The Shadow of the Supermassive Black Hole. *Astrophys. J.* **875**, L1 (2019). 1906.11238.

[109] Johannsen, T. *et al.* Testing General Relativity with the Shadow Size of Sgr A*. *Phys. Rev. Lett.* **116**, 031101 (2016). 1512.02640.

[110] Gendreau, K. C., Arzoumaniana, Z. & Okajimaa, T. The Neutron star Interior Composition ExploreR (NICER): an Explorer mission of opportunity for soft x-ray timing spectroscopy. URL `https://heasarc.gsfc.nasa.gov/docs/nicer/papers/NICER-SPIE-July2012-v4.pdf`.

[111] Cardenas-Avendano, A., Nampalliwar, S. & Yunes, N. Gravitational-wave versus X-ray tests of strong-field gravity. *Class. Quant. Grav.* **37**, 135008 (2020). 1912.08062.

[112] Belgacem, E., Dirian, Y., Foffa, S. & Maggiore, M. Modified gravitational-wave propagation and standard sirens. *Phys. Rev. D* **98**, 023510 (2018). 1805.08731.

[113] Pardo, K., Fishbach, M., Holz, D. E. & Spergel, D. N. Limits on the number of spacetime dimensions from GW170817. *JCAP* **07**, 048 (2018). 1801.08160.

[114] Alexander, S. & Yunes, N. Chern-Simons Modified General Relativity. *Phys. Rept.* **480**, 1–55 (2009). 0907.2562.

[115] Alexander, S. H. & Yunes, N. Gravitational wave probes of parity violation in compact binary coalescences. *Phys. Rev. D* **97**, 064033 (2018). 1712.01853.

[116] Isi, M. & Weinstein, A. J. Probing gravitational wave polarizations with signals from compact binary coalescences (2017). 1710.03794.

[117] Lattimer, J. M. The nuclear equation of state and neutron star masses. *Ann. Rev. Nucl. Part. Sci.* **62**, 485–515 (2012). 1305.3510.

[118] Baiotti, L. Gravitational waves from neutron star mergers and their relation to the nuclear equation of state. *Prog. Part. Nucl. Phys.* **109**, 103714 (2019). 1907.08534.

[119] Hewish, A., Bell, S., Pilkington, J., Scott, P. & Collins, R. Observation of a rapidly pulsating radio source. *Nature* **217**, 709–713 (1968).

[120] Bauswein, A. *et al.* Identifying a first-order phase transition in neutron star mergers through gravitational waves. *Phys. Rev. Lett.* **122**, 061102 (2019). 1809.01116.

[121] Most, E. R. *et al.* On the deconfinement phase transition in neutron-star mergers. *Eur. Phys. J. A* **56**, 59 (2020). 1910.13893.

[122] Baumgarte, T. W., Shapiro, S. L. & Shibata, M. On the maximum mass of differentially rotating neutron stars. *Astrophys. J. Lett.* **528**, L29 (2000). astro-ph/9910565.

[123] Kastaun, W. & Galeazzi, F. Properties of hypermassive neutron stars formed in mergers of spinning binaries. *Phys. Rev. D* **91**, 064027 (2015). 1411.7975.

[124] Flanagan, E. E. & Hinderer, T. Constraining neutron star tidal Love numbers with gravitational wave detectors. *Phys. Rev. D* **77**, 021502 (2008). 0709.1915.

[125] Xing, Z.-G., Centrella, J. M. & McMillan, S. L. Gravitational radiation from coalescing binary neutron stars. *Phys. Rev. D* **50**, 6247–6261 (1994). gr-qc/9411029.

[126] Read, J. S. *et al.* Matter effects on binary neutron star waveforms. *Phys. Rev. D* **88**, 044042 (2013). 1306.4065.

[127] Bauswein, A. & Janka, H.-T. Measuring neutron-star properties via gravitational waves from binary mergers. *Phys. Rev. Lett.* **108**, 011101 (2012). 1106.1616.

[128] Takami, K., Rezzolla, L. & Baiotti, L. Constraining the Equation of State of Neutron Stars from Binary Mergers. *Phys. Rev. Lett.* **113**, 091104 (2014). 1403.5672.

[129] Cardoso, V. & Pani, P. Testing the nature of dark compact objects: a status report. *Living Rev. Rel.* **22**, 4 (2019). 1904.05363.

[130] Scherrer, R. J. & Turner, M. S. On the Relic, Cosmic Abundance of Stable Weakly Interacting Massive Particles. *Phys. Rev. D* **33**, 1585 (1986). [Erratum: Phys.Rev.D 34, 3263 (1986)].

[131] Kim, J. E. & Carosi, G. Axions and the Strong CP Problem. *Rev. Mod. Phys.* **82**, 557–602 (2010). [Erratum: Rev.Mod.Phys. 91, 049902 (2019)], 0807.3125.

[132] Barack, L. *et al.* Black holes, gravitational waves and fundamental physics: a roadmap. *Class. Quant. Grav.* **36**, 143001 (2019). 1806.05195.

[133] Arvanitaki, A., Dimopoulos, S., Dubovsky, S., Kaloper, N. & March-Russell, J. String Axi-

verse. *Phys. Rev. D* **81**, 123530 (2010). 0905.4720.

[134] Brito, R. *et al.* Gravitational wave searches for ultralight bosons with LIGO and LISA. *Phys. Rev. D* **96**, 064050 (2017). 1706.06311.

[135] Zel'dovich, Y. Generation of waves by a rotating body. *Pis'ma Zh. Eksp. Teor. Fiz., JETP Lett.* **14**, 270 (1971).

[136] Penrose, R. & Floyd, R. M. Extraction of rotational energy from a black hole. *Nature Physical Science* **229**, 177–179 (1971).

[137] Carr, B. & Kuhnel, F. Primordial Black Holes as Dark Matter: Recent Developments (2020). 2006.02838.

[138] Krolak, A. & Schutz, B. F. Coalescing binaries - probe of the universe. *General Relativity and Gravitation* **19**, 1163–1171 (1987).

[139] Dhawan, S., Bulla, M., Goobar, A., Carracedo, A. S. & Setzer, C. N. Constraining the observer angle of the kilonova AT2017gfo associated with GW170817: Implications for the hubble constant. *The Astrophysical Journal* **888**, 67 (2020).

[140] Abbott, B. *et al.* A gravitational-wave measurement of the Hubble constant following the second observing run of Advanced LIGO and Virgo (2019). 1908.06060.

[141] Feeney, S. M., Mortlock, D. J. & Dalmasso, N. Clarifying the Hubble constant tension with a Bayesian hierarchical model of the local distance ladder. *Mon Not R astr Soc* **476**, 3861–3882 (2018). 1707.00007.

[142] Feeney, S. M. *et al.* Prospects for resolving the Hubble constant tension with standard sirens. *ArXiv e-prints* (2018). 1802.03404.

[143] Copeland, E. J., Sami, M. & Tsujikawa, S. Dynamics of dark energy. *International Journal of Modern Physics D* **15**, 1753–1935 (2006).

[144] Del Pozzo, W., Sesana, A. & Klein, A. Stellar binary black holes in the LISA band: a new class of standard sirens. *Monthly Notices of the Royal Astronomical Society* **475**, 3485–3492 (2018). 1703.01300.

[145] MacLeod, C. L. & Hogan, C. J. Precision of Hubble constant derived using black hole binary absolute distances and statistical redshift information. *Physical Review D* **77**, 043512 (2008). 0712.0618.

[146] Tamanini, N. *et al.* Science with the space-based interferometer eLISA. III: probing the expansion of the universe using gravitational wave standard sirens. *Journal of Cosmology*

*and Astroparticle Physics* **4**, 002 (2016). 1601.07112.

[147] Grishchuk, L. P. REVIEWS OF TOPICAL PROBLEMS: Relic gravitational waves and cosmology. *Physics Uspekhi* **48**, 1235–1247 (2005). gr-qc/0504018.

[148] Lasky, P. D. *et al.* Gravitational-Wave Cosmology across 29 Decades in Frequency. *Physical Review X* **6**, 011035 (2016). 1511.05994.

[149] Gerosa, D. *et al.* Multiband gravitational-wave event rates and stellar physics. *Physical Review D* **99** (2019).

[150] Lamberts, A. *et al.* Predicting the LISA white dwarf binary population in the milky way with cosmological simulations. *Monthly Notices of the Royal Astronomical Society* **490**, 5888–5903 (2019).

[151] Katz, M. L. *et al.* Probing massive black hole binary populations with LISA. *Monthly Notices of the Royal Astronomical Society* (2019).

[152] Amaro-Seoane, P. *et al.* Intermediate and extreme mass-ratio inspirals—astrophysics, science applications and detection using LISA. *Classical and Quantum Gravity* **24**, R113–R169 (2007).

[153] Klein, A. *et al.* Science with the space-based interferometer eLISA: Supermassive black hole binaries. *Phys. Rev. D* **93**, 024003 (2016). 1511.05581.

[154] Taylor, S. R., van Haasteren, R. & Sesana, A. From bright binaries to bumpy backgrounds: Mapping realistic gravitational wave skies with pulsar-timing arrays 2006.04810v1.

[155] Savchenko, V. *et al.* INTEGRAL Detection of the First Prompt Gamma-Ray Signal Coincident with the Gravitational-wave Event GW170817. *Astrophys. J. Lett.* **848**, L15 (2017). 1710.05449.

[156] Cowperthwaite, P. *et al.* The Electromagnetic Counterpart of the Binary Neutron Star Merger LIGO/Virgo GW170817. II. UV, Optical, and Near-infrared Light Curves and Comparison to Kilonova Models. *Astrophys. J. Lett.* **848**, L17 (2017). 1710.05840.

[157] Alexander, K. *et al.* The Electromagnetic Counterpart of the Binary Neutron Star Merger LIGO/VIRGO GW170817. VI. Radio Constraints on a Relativistic Jet and Predictions for Late-Time Emission from the Kilonova Ejecta. *Astrophys. J. Lett.* **848**, L21 (2017). 1710.05457.

[158] Drout, M. *et al.* Light Curves of the Neutron Star Merger GW170817/SSS17a: Implications for R-Process Nucleosynthesis. *Science* **358**, 1570–1574 (2017). 1710.05443.

[159] De, S. *et al.* Tidal Deformabilities and Radii of Neutron Stars from the Observation of GW170817. *Phys. Rev. Lett.* **121**, 091102 (2018). [Erratum: Phys.Rev.Lett. 121, 259902 (2018)], 1804.08583.

[160] Abbott, B. *et al.* GW170817: Measurements of neutron star radii and equation of state. *Phys. Rev. Lett.* **121**, 161101 (2018). 1805.11581.

[161] Most, E. R., Weih, L. R., Rezzolla, L. & Schaffner-Bielich, J. New constraints on radii and tidal deformabilities of neutron stars from GW170817. *Phys. Rev. Lett.* **120**, 261103 (2018). 1803.00549.

[162] Radice, D., Perego, A., Zappa, F. & Bernuzzi, S. GW170817: Joint Constraint on the Neutron Star Equation of State from Multimessenger Observations. *Astrophys. J. Lett.* **852**, L29 (2018). 1711.03647.

[163] Troja, E. *et al.* The outflow structure of GW170817 from late-time broad-band observations. *Mon. Not. Roy. Astron. Soc.* **478**, L18–L23 (2018). 1801.06516.

[164] Bauswein, A., Just, O., Janka, H.-T. & Stergioulas, N. Neutron-star radius constraints from GW170817 and future detections. *Astrophys. J. Lett.* **850**, L34 (2017). 1710.06843.

[165] Waxman, E., Ofek, E. O., Kushnir, D. & Gal-Yam, A. Constraints on the ejecta of the GW170817 neutron-star merger from its electromagnetic emission. *Mon. Not. Roy. Astron. Soc.* **481**, 3423–3441 (2018). 1711.09638.

[166] Metzger, B. D., Thompson, T. A. & Quataert, E. A magnetar origin for the kilonova ejecta in GW170817. *Astrophys. J.* **856**, 101 (2018). 1801.04286.

[167] Hajela, A. *et al.* Two Years of Nonthermal Emission from the Binary Neutron Star Merger GW170817: Rapid Fading of the Jet Afterglow and First Constraints on the Kilonova Fastest Ejecta. *Astrophys. J. Lett.* **886**, L17 (2019). 1909.06393.

[168] Lattimer, J. Impact of GW170817 for the nuclear physics of the EOS and the r-process. *Annals Phys.* **411**, 167963 (2019).

[169] Lazzati, D. *et al.* Late time afterglow observations reveal a collimated relativistic jet in the ejecta of the binary neutron star merger GW170817. *Phys. Rev. Lett.* **120**, 241103 (2018). 1712.03237.

[170] Ivezic, Z. *et al.* Large Synoptic Survey Telescope: From Science Drivers To Reference Design. *Serbian Astronomical Journal* **176**, 1–13 (2008).

[171] Kalirai, J. Scientific discovery with the James Webb Space Telescope. *Contemporary Physics*

**59**, 251–290 (2018). 1805.06941.

[172] Gullieuszik, M., Falomo, R., Greggio, L., Uslenghi, M. & Fantinel, D. Exploring high-z galaxies with the E-ELT. *A&A* **593**, A24 (2016). 1607.02950.

[173] McCarthy, P. J. *et al.* Overview and status of the giant magellan telescope project. In Gilmozzi, R., Marshall, H. K. & Spyromilio, J. (eds.) *Ground-based and Airborne Telescopes VII* (SPIE, 2018).

[174] Skidmore, W., Anupama, G. C. & Srianand, R. The thirty meter telescope international observatory facilitating transformative astrophysical science. *Current Science* **113**, 639 (2017).

[175] Gehrels, N. *et al.* The swift gamma-ray burst mission. *The Astrophysical Journal* **611**, 1005 (2004).

[176] Meegan, C. *et al.* The fermi gamma-ray burst monitor. *The Astrophysical Journal* **702**, 791 (2009).

[177] Winkler, C. *et al.* The integral mission. *Astronomy & Astrophysics* **411**, L1–L6 (2003).

[178] Merloni, A. *et al.* erosita science book: Mapping the structure of the energetic universe 1209.3114v2.

[179] Yuan, W. *et al.* Einstein Probe - a small mission to monitor and explore the dynamic X-ray Universe. *arXiv e-prints* arXiv:1506.07735 (2015). 1506.07735.

[180] Brandt, S. K. *et al.* The wide field monitor onboard the eXTP mission. In den Herder, J.-W. A., Nakazawa, K. & Nikzad, S. (eds.) *Space Telescopes and Instrumentation 2018: Ultraviolet to Gamma Ray* (SPIE, 2018).

[181] Wei, J. *et al.* The deep and transient universe in the svom era: New challenges and opportunities - scientific prospects of the svom mission 1610.06892v1.

[182] McEnery, J. E. *et al.* All-sky medium energy gamma-ray observatory: Exploring the extreme multimessenger universe. *arXiv preprint arXiv:1907.07558* (2019).

[183] Willingale, R., Pareschi, G., Christensen, F. & den Herder, J.-W. The hot and energetic universe: The optical design of the athena+ mirror 1307.1709v1.

[184] Bautz, M. W. The lynx x-ray observatory: Science drivers. In Siegmund, O. H. (ed.) *UV, X-Ray, and Gamma-Ray Space Instrumentation for Astronomy XXI* (SPIE, 2019).

[185] Amati, L. *et al.* The THESEUS space mission concept: science case, design and expected performances. *Advances in Space Research* **62**, 191–244 (2018). 1710.04638.

[186] Camp, J. *et al.* Transient Astrophysics Probe. In *BAAS*, vol. 51, 85 (2019).

[187] Dewdney, P., Hall, P., Schilizzi, R. & Lazio, T. The square kilometre array. *Proceedings of the IEEE* **97**, 1482–1496 (2009).

[188] McKinnon, M. *et al.* ngVLA: The Next Generation Very Large Array. In *Bulletin of the American Astronomical Society*, vol. 51, 81 (2019).

[189] Totani, T. Cosmological fast radio bursts from binary neutron star mergers 1307.4985v3.

[190] Acharya, B. *et al.* Introducing the CTA concept. *Astroparticle Physics* **43**, 3–18 (2013).

[191] Ando, S. *et al.* Colloquium: Multimessenger astronomy with gravitational waves and high-energy neutrinos. *Reviews of Modern Physics* **85**, 1401 (2013).

[192] Barnes, J. E. & Hernquist, L. E. Fueling starburst galaxies with gas-rich mergers. *The Astrophysical Journal Letters* **370**, L65–L68 (1991).

[193] Schnittman, J. D. Electromagnetic counterparts to black hole mergers. *Classical and Quantum Gravity* **28**, 094021 (2011). 1010.3250.

[194] Gold, R. *et al.* Accretion disks around binary black holes of unequal mass: General relativistic MHD simulations of postdecoupling and merger. *Physical Review D* **90**, 104030 (2014). 1410.1543.

[195] Bowen, D. B. *et al.* Quasi-periodic Behavior of Mini-disks in Binary Black Holes Approaching Merger. *The Astrophysical Journal Letters* **853**, L17 (2018). 1712.05451.

[196] Littenberg, T. *et al.* Gravitational wave survey of galactic ultra compact binaries. *BAAS* **51**, 34 (2019).

[197] Kupfer, T. *et al.* LISA verification binaries with updated distances from Gaia Data Release 2. *MNRAS* **480**, 302–309 (2018). 1805.00482.

[198] Burdge, K. B. *et al.* General relativistic orbital decay in a seven-minute-orbital-period eclipsing binary system. *Nature* **571**, 528–531 (2019).

[199] Collaboration, G. The gaia mission 1609.04153v1.

[200] Ivezić, Ž. *et al.* LSST: From science drivers to reference design and anticipated data products. *The Astrophysical Journal* **873**, 111 (2019).

[201] Dotti, M., Sesana, A. & Decarli, R. Massive Black Hole Binaries: Dynamical Evolution and Observational Signatures. *Advances in Astronomy* **2012**, 940568 (2012). 1111.0664.

[202] Tanaka, T. L. & Haiman, Z. Electromagnetic signatures of supermassive black hole binaries resolved by PTAs. *Classical and Quantum Gravity* **30**, 224012 (2013). 1309.2302.

[203] Haiman, Z., Kocsis, B. & Menou, K. The Population of Viscosity- and Gravitational Wave-

driven Supermassive Black Hole Binaries Among Luminous Active Galactic Nuclei. *The Astrophysical Journal* **700**, 1952–1969 (2009). 0904.1383.

[204] Smits, R., Tingay, S. J., Wex, N., Kramer, M. & Stappers, B. Prospects for accurate distance measurements of pulsars with the square kilometre array: Enabling fundamental physics. *Astronomy & Astrophysics* **528**, A108 (2011).

[205] Lee, K. J. *et al.* Gravitational wave astronomy of single sources with a pulsar timing array. *Monthly Notices of the Royal Astronomical Society* **414**, 3251–3264 (2011).

[206] Collaboration, L. S. *et al.* Gravitational wave astronomy with ligo and similar detectors in the next decade. *arXiv preprint arXiv:1904.03187* (2019).

[207] Abbott, B. P. *et al.* Prospects for observing and localizing gravitational-wave transients with advanced ligo, advanced virgo and kagra. *Living Reviews in Relativity* **21**, 3 (2018).

[208] McCuller, L. *et al.* Frequency-dependent squeezing for advanced ligo. *Physical Review Letters* **124**, 171102 (2020).

[209] Stefszky, M. *et al.* Balanced homodyne detection of optical quantum states at audio-band frequencies and below. *Classical and Quantum Gravity* **29**, 145015 (2012).

[210] Fritschel, P., Evans, M. & Frolov, V. Balanced homodyne readout for quantum limited gravitational wave detectors. *Optics express* **22**, 4224–4234 (2014).

[211] Kim, D. S. *et al.* Nuclear quantum effect with pure anharmonicity and the anomalous thermal expansion of silicon. *Proceedings of the National Academy of Sciences* **115**, 1992–1997 (2018).

[212] Schnabel, R. *et al.* Building blocks for future detectors: Silicon test masses and 1550 nm laser light. *Journal of Physics: Conference Series* **228**, 012029 (2010).

[213] Vajente, G. *et al.* Method for the experimental measurement of bulk and shear loss angles in amorphous thin films. *Physical Review D* **101** (2020).

[214] Cole, G. D., Zhang, W., Martin, M. J., Ye, J. & Aspelmeyer, M. Tenfold reduction of brownian noise in high-reflectivity optical coatings. *Nature Photonics* **7**, 644 (2013).

[215] Oelker, E. *et al.* Audio-band frequency-dependent squeezing for gravitational-wave detectors. *Physical review letters* **116**, 041102 (2016).

[216] Wellmann, F. *et al.* Low-noise, single-frequency 200 w fiber amplifier. In Dong, L. & Zervas, M. N. (eds.) *Fiber Lasers XVII: Technology and Systems* (SPIE, 2020).

[217] Harms, J. Terrestrial gravity fluctuations. *Living Reviews in Relativity* **22** (2019).

[218] Hall, E. D. & Evans, M. Metrics for next-generation gravitational-wave detectors. *Class.*

*Quant. Grav.* **36**, 225002 (2019). 1902.09485.

[219] Dylla, H. F., Weiss, R. & Zucker, M. E. Proceedings: NSF Workshop on Large Ultrahigh-Vacuum Systems for Frontier Scientific Research. Tech. Rep. P1900007-v1, LIGO Laboratory (2019).

[220] Ackley, K. *et al.* Neutron star extreme matter observatory: A kilohertz-band gravitational-wave detector in the global network (2020). 2007.03128.

[221] THE SPACE DEPARTMENT, S. O., THE GUIDANCE, S. O. & LABORATORY, C. A satellite freed of all but gravitational forces: "triad i". *Journal of Spacecraft and Rockets* **11**, 637–644 (1974).

[222] Armano, M. *et al.* Sub-Femto-g Free Fall for Space-Based Gravitational Wave Observatories: LISA Pathfinder Results. *Phys. Rev. Lett.* **116**, 231101 (2016).

[223] Armano, M. *et al.* Beyond the Required LISA Free-Fall Performance: New LISA Pathfinder Results down to 20 $\mu$ Hz. *Phys. Rev. Lett.* **120**, 061101 (2018).

[224] Armstrong, J., Estabrook, F. & Tinto, M. Time-delay interferometry for space-based gravitational wave searches. *The Astrophysical Journal* **527**, 814–826 (1999).

[225] Shaddock, D., Ware, B., Spero, R. & Vallisneri, M. Post-process time delay interferometry for LISA. *Physical Review D* **70** (2004).

[226] Vallisneri, M. Synthetic LISA: Simulating time delay interferometry in a model LISA. *Phys. Rev. D* **71**, 022001 (2005). gr-qc/0407102.

[227] de Vine, G. *et al.* Experimental Demonstration of Time-Delay Interferometry for the Laser Interferometer Space Antenna. *Phys. Rev. Lett.* **104**, 211103 (2010). 1005.2176.

[228] Mitryk, S. J., Mueller, G. & Sanjuan, J. Hardware-based demonstration of time-delay interferometry and TDI-ranging with spacecraft motion effects. *Phys. Rev. D* **86**, 122006 (2012). 1205.1934.

[229] Abich, K. *et al.* In-Orbit Performance of the GRACE Follow-on Laser Ranging Interferometer. *Phys. Rev. Lett.* **123**, 031101 (2019). 1907.00104.

[230] Luo, J. *et al.* TianQin: a space-borne gravitational wave detector. *Classical and Quantum Gravity* **33**, 035010 (2016).

[231] Hu, W.-R. & Wu, Y.-L. The Taiji Program in Space for gravitational wave physics and the nature of gravity. *National Science Review* **4**, 685–686 (2017). URL `https://doi.org/10.1093/nsr/nwx116`. https://academic.oup.com/nsr/article-pdf/4/5/685/31566708/nwx116.pdf.

[232] Arca Sedda, M. *et al.* The Missing Link in Gravitational-Wave Astronomy: Discoveries waiting in the decihertz range. *arXiv e-prints* arXiv:1908.11375 (2019). 1908.11375.

[233] Kawamura, S. *et al.* Space Gravitational Wave Antenna DECIGO and B-DECIGO. *Int. J. Mod. Phys. D* **28**, 1845001 (2019).

[234] Kawamura, S. *et al.* Current status of space gravitational wave antenna decigo and b-decigo 2006.13545v1.

[235] Sesana, A. *et al.* Unveiling the Gravitational Universe at $\mu$-Hz Frequencies. *arXiv e-prints* arXiv:1908.11391 (2019). 1908.11391.

[236] Baibhav, V. *et al.* Probing the Nature of Black Holes: Deep in the mHz Gravitational-Wave Sky. *arXiv e-prints* arXiv:1908.11390 (2019). 1908.11390.

[237] Baker, J. *et al.* High angular resolution gravitational wave astronomy. *arXiv e-prints* arXiv:1908.11410 (2019). 1908.11410.

[238] Hobbs, G. *et al.* An ultra-wide bandwidth (704 to 4 032 MHz) receiver for the Parkes radio telescope. *Publications of the Astronomical Society of the Pacific* **37**, e012 (2020). 1911.00656.

[239] Vallisneri, M. *et al.* Modeling the Uncertainties of Solar System Ephemerides for Robust Gravitational-wave Searches with Pulsar-timing Arrays. *ApJ* **893**, 112 (2020). 2001.00595.

[240] Janssen, G. *et al.* Gravitational Wave Astronomy with the SKA. *Advancing Astrophysics with the Square Kilometre Array (AASKA14)* 37 (2015). 1501.00127.

## ACKNOWLEDGEMENTS

The authors gratefully acknowledge the following support: M. Bailes and D. McClelland are supported by Australian Research Council under the ARC Centre of Excellence for Gravitational Wave Discovery grant CE170100004. D. D. McClelland also acknowledges the support of the ARC Linkage Infrastructure, Equipment and Facilities grant LE170100217. M. Branchesi and S. Katsanevas acknowledge the support of the European Union's Horizon 2020 Programme under the AHEAD2020 Project grant agreement 871158. S. Katsanevas is also supported by Université de Paris, France. M. Evans, A. Lazzarini, D. Reitze, and D. Shoemaker are supported by the National Science Foundation (NSF) LIGO Laboratory award PHY-1764464. M. Evans also acknowledges support from NSF award PHY-1836814. T. Kajita, H. Shinkai, and Y. Saito acknowledge support as members of KAGRA supported

by MEXT and JSPS in Japan, NRF and Computing Infrastructure Project of KISTI-GSDC in Korea, and MoST and Academia Sinica in Taiwan. L. Lehner is supported in part by CIFAR, NSERC through a Discovery grant, and by Perimeter Institute for Theoretical Physics. Research at Perimeter Institute is supported by the Government of Canada and by the Province of Ontario through the Ministry of Research, Innovation and Science. G. Losurdo, M. Punturo, and F. Ricci acknowledge the Italian Istituto Nazionale di Fisica Nucleare (INFN), the French Centre National de la Recherche Scientifique (CNRS), and the Foundation for Fundamental Research on Matter supported by the Netherlands Organisation for Scientific Research, for the construction and operation of the Virgo detector and the creation and support of the EGO consortium. The authors also gratefully acknowledge research support from these agencies as well as by the Italian Ministry of University and Research (MIUR) for the support to the study and design of Einstein Telescope. H. Lück is supported by the Max Planck Society, Leibniz Universität Hannover, and Deutsche Forschungsgemeinschaft under Germany's Excellence Strategy EXC2123 Quantum Frontiers program. S. Ransom is a CIFAR Fellow at the National Radio Astronomy Observatory (NRAO). NRAO is a facility of the National Science Foundation operated under cooperative agreement by Associated Universities, Inc. S. Ransom and X. Siemens are also supported as members of NANOGrav and SMR by the NSF Physics Frontiers Center award PHY-1430284. B. S. Sathyaprakash is supported in part by NSF awards PHY-1836779, AST-1716394 and AST-1708146. B. Schutz cknowledges support from the Science and Technology Facilities Council (STFC) of the United Kingdom. A. Sesana is supported by the European Research Council (ERC) under the European Union's Horizon 2020 research and innovation program ERC-2018-COG under grant 818691 (B Massive). J. I. Thorpe acknowledges the support of the U.S. National Aeronautics and Space Administration (NASA). J. van den Brand is supported by the Foundation for Fundamental Research on Matter supported by the Netherlands Organisation for Scientific Research. S. Vitale is supported by the Agenzia Spaziale Italiana and INFN.

## COMPETING INTERESTS

The authors declare that they have no competing financial interests.

## CORRESPONDENCE

Correspondence and requests for materials should be addressed to D. H. Reitze (email: dreitze@caltech.edu).